Challenges with Developing a Measurement-Based Basin Methane Intensity Estimate: A Case Study from the Haynesville

Kristian D. Hajny[1], Bailey K. Fosdick[1], Zachary Weller[1], Ella Martinez[1], Hon Xing Wong[1], Abigail Corbett[1], Christopher Moore[1,]*

[1] GTI Energy

[*]Christopher Moore – GTI Energy, 1700 S Mount Prospect Rd., Des Plaines, IL, 60018; Email: cmoore@gti.energy

KEYWORDS

Methane, methane intensity, measurement-based inventory, greenhouse gas inventory, oil and gas, Haynesville Basin

SYNOPSIS

We present methane emissions and emissions intensity estimates for upstream and midstream oil and gas activities in the Haynesville Basin in 2024 and demonstrate how key methodological decisions that are not standardized across reporting frameworks influence these calculations.

ABSTRACT

Methane intensity, the emissions relative to production, has been a focus in global regulations on oil and gas production and imports, given the climate benefits of methane emission reductions. Methodological frameworks to create annual measurement-based emissions inventory estimates and calculate methane intensity using snapshot measurements have been developed. However, there are still multiple decision points within these frameworks whose impact may be underappreciated. These include uncertainty in the underlying facility population and associated production in purview. In this work, we discuss the development of a comprehensive measurement-based inventory for the dry gas Haynesville Basin located in the U.S. States of Texas and Louisiana using Bridger Photonics LiDAR data. From a measurement dataset covering 8% of all facilities, we estimate annual basin total methane emissions of 760 [610, 940] Gg/year and a methane intensity of 0.79% [0.63%, 0.98%] (95% confidence intervals), in agreement with previous measurement-based studies in the region. We then show that different methodological choices can result in a difference of more than a factor of two in the estimated methane intensity for the subset of choices considered in this work. As such, this work demonstrates the importance of considering all aspects of the methodology to produce comparable methane intensity estimates.

1. Introduction

Oil and gas (O&G) production activities are estimated to represent 18% of United States (U.S.) methane (CH_4) emissions in 2022,[1] and reducing these emissions has been discussed as a cost-effective means to mitigate climate impacts, especially in the short term. This is because CH_4 has a high global warming potential and short lifetime relative to that of carbon dioxide (CO_2).[2] There has been significant research activity focused on accurately quantifying emissions to better understand emission reduction progress and identify opportunities for further emissions

mitigation.[3–7] Alongside this research is a growing body of international regulations and commitments that support O&G operators' actions to mitigate emissions.[8–12] CH_4 is often quantified by the O&G industry not only in terms of emissions, but also as a CH_4 intensity—the emissions normalized by production.[13–18] This metric enables more useful comparisons across time and space and is often a target for regulations as it accounts for energy production. For example, CH_4 intensity has been used to understand the comparative performance across sectors (e.g., production, transmission)[19] and as part of lifecycle analyses, which incorporate CH_4 intensity estimates for production, to compare different fuels (e.g., natural gas, coal).[20–22]

Within the O&G sector in recent years, CH_4 intensity has played an increasing role in international regulations,[8–12] academic studies, voluntary reporting,[15–17,23] and reduction targets. Voluntary reporting or certification frameworks assist operators in producing reliable CH_4 emissions and CH_4 intensity estimates (e.g., ONE Future[15], MiQ[17], Veritas[16], Oil and Gas Methane Partnership (OGMP) 2.0[23]). Frameworks can focus on absolute emissions reduction goals, CH_4 intensity thresholds, or both. Research on lifecycle emissions, including CH_4 intensity data, also recently influenced U.S. policy regarding liquified natural gas.[20–22,24,25] Recent legislation from the European Union (EU) imposes CH_4 intensity requirements for domestic and imported natural gas using methods akin to OGMP 2.0 Level 5 reporting[23], requiring independent measurements, starting in 2030.[18] However, enforcement of such requirements may be difficult, particularly in the U.S. where natural gas is comingled across many operators between the point of production and point of sale. Given the comingling of natural gas across operators within a single basin, CH_4 intensity estimates for the entire basin allow operators to perform important benchmarking comparisons to the basin-wide intensity estimate. Calculating accurate and transparent CH_4

intensities is critical given the metric's importance; however, both the CH_4 emissions estimate and production inputs present several challenges.

While methane emission estimates were traditionally developed using emission factor-based approaches, there are now widespread efforts to use measurements for this purpose. There are several approaches for using measurements to create emission estimates, and these approaches have been applied at different spatial scales (e.g., operator level, basin level, national level). Numerous recent studies discuss how to develop emissions inventories, extrapolating measurements to appropriately account for unmeasured sites, emissions too small to have been detected, and across time to an annual estimate.[5,26–30] These approaches must also account for the potential impact of short-lived, large emission events that can strongly skew the emission distribution.[3,6,31,32] While previous studies have discussed the complex process of extrapolating measured emissions to represent an annual inventory at the basin scale and the potential uncertainties associated with this process,[5,26–30] there is no standard approach for developing these estimates.

Adding to the estimation challenges are the multiple definitions of CH_4 intensity. Some methodologies weight the emissions to account for emissions due to co-produced oil while others use only the CH_4 content of produced natural gas as the divisor. Furthermore, production can be defined in several ways.[3,13,33–36] CH_4 intensity is sometimes referred to as a leak rate, a CH_4 loss rate, or an energy intensity when expressed in energy units (e.g., g/MJ), though these may represent somewhat different metrics depending on the calculation method used.[33,36] While many reporting frameworks are explicit about their calculation method, the large overlap in units and terminology across methods can still lead to confusion.[33,36]

Further complicating this metric, a CH_4 intensity can be calculated at various spatial scales (e.g., facility, operator, basin, national), and the population of facilities within a given geographic area or spatial target scope may not be clearly defined. Sherwin et al.[37] discussed the impact of spatial scale by calculating a Permian Basin CH_4 intensity of 4.6% [4.4%, 4.9%] (95% confidence interval), but showing that the Delaware and Midland sub-basins were markedly different at 3.4% [3.2%, 3.6%] and 8.5% [7.8%, 9.4%], respectively. The lack of standardization across these complexities is consequential for the scientific community, reporting frameworks, operators, and regulators, as it makes inappropriate comparisons far more likely. Decision makers require consistent, directly comparable CH_4 intensity estimates to effectively support their emissions reduction efforts.

While several studies have examined the impacts of individual methodological decision points when calculating methane intensity, we for the first time provide a study examining the combined effects of these inputs at the basin scale and recommend how the impact can be mitigated. We accomplish this using a large dataset collected by Bridger Photonics Inc. (Bridger) to develop a comprehensive measurement-based inventory for the Haynesville Basin in 2024. We refer to the inventory as 1) measurement-based, as it relies exclusively on Bridger measurement data, and 2) comprehensive, as we use extrapolation methods to ensure the inventory reflects emissions of all sizes across the entire basin for the year 2024. Similar extrapolation methods have been discussed in a recent companion paper,[30] so we instead focus here on other aspects of the methodology that can influence the resulting CH_4 intensity estimate. As CH_4 intensity is being considered in regulations,[18,38] it is especially important that these differences be understood and accounted for. We present an initial estimate of both total CH_4 emissions and CH_4 intensity for the basin that can be directly compared to values in the literature, then discuss the impacts that basin definition,

activity data, calculation method, and production data can have in subsequent analyses. We conclude with a summary of the methodological details we believe could significantly affect a CH_4 intensity estimate and therefore should be provided along with a CH_4 intensity for improved transparency and comparability.

2. Methods

2.1. Study Area

The Haynesville Basin is a U.S. dry gas basin encompassing parts of northeast Texas and northwest Louisiana. According to the Energy Information Administration (EIA), it marketed 12.4 billion cubic feet per day (BCF/d) in 2024, making it the third most productive U.S. natural gas basin, behind only the Permian and Marcellus basins.[39] In the initial analysis, we define the Haynesville Basin as the 18 counties in the EIA 2022 county code master list, as shown in Figure 1 and listed in Supporting Information (SI) Table S1.[40] In secondary analyses, we also considered the Haynesville play as provided by Enverus™[,41] in the “play" variable of the wells dataset, which is defined using Enverus-defined shapefiles and location, date, trajectory, and formation criteria to determine the likely geological formation a well is accessing.

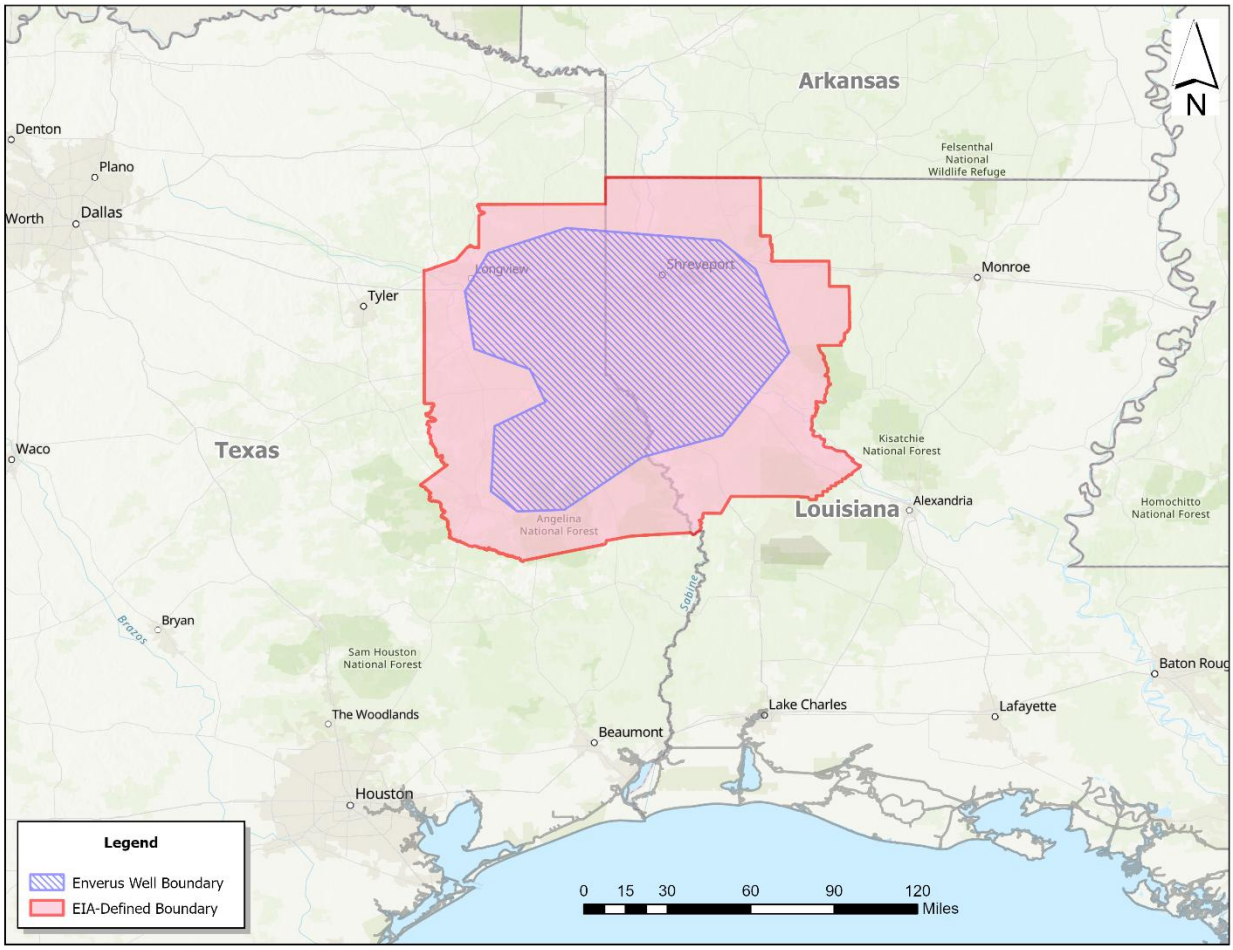

Figure 1. Map[42] with the Haynesville Basin outline according to the EIA-based boundary shown in red and the boundary according to the Enverus definition shown as a blue hatched area.

2.2. Measurement and Population Data

Bridger conducted aerial surveys to obtain emissions measurements from a subset of facilities in the basin. Bridger's Gas Mapping LiDAR (GML) combines LiDAR topography and path-integrated CH_4 concentration measurements with navigation and photographic data to create geo-registered plume imagery, emission source location estimates, snapshot emission rate estimates, and labels for major pieces of equipment within each facility. They deploy GML from a small, human-piloted aircraft, and their method has been thoroughly described and characterized in the

literature.[43–46] They reported an average 90% Probability of Detection (POD) emission rate of 1.27 kg/h in 2023 using a model developed with controlled release data using a combination of gas concentration noise and wind speed to estimate POD.[45] While recent work has suggested that POD models developed from controlled release tests may underestimate small emissions in field conditions and underestimate the impact of wind speed, no alternative method to estimate POD is currently available.[47]

We collaborated with Bridger to develop a sampling plan to build a comprehensive measurement-based inventory for the basin, including all production and non-pipeline midstream sources within the basin boundaries. Though Bridger can measure at the source-level, all data in this work were provided at the facility level. This work also did not include measurements of pipeline emissions, which Sherwin et al.[37] observed represented up to 33% of total emissions across their campaigns. Facilities were stratified into compressor stations, gas processing plants, non-producing facilities, and well sites. Well sites were further stratified into those with marginal (0-15 barrels of oil equivalent per day, BOED), standard (15 - 300 BOED), and high (≥300 BOED) production, as previous literature has reported a correlation, albeit weak, between CH_4 emissions and natural gas production.[48–51] Bridger estimated the population count of non-producing facilities was 5.2% of producing facilities based on previous measurements that they made in the Haynesville Basin. Non-producing facilities tend to have non-well equipment and do not clearly belong to other strata, e.g., tank batteries.

Table 1 lists the facility population counts for each stratum in the initial analysis using values provided by Bridger, who relied partly on data from Rextag™[,52]. Table S2 provides equivalent information based on the Enverus population data used in secondary analyses. As both Enverus and Rextag are commercial products, their detailed methods are not publicly available and may

change over time. As such, we cannot detail why these products differ but still use them as two example datasets to demonstrate the issue of inconsistent/uncertain population data. There are also other datasets, such as state reports or operator records, that could be used and likely also differ. All Enverus data was filtered to include only active facilities with production in 2024. As Enverus only provides well data, while Rextag also includes gas processing plants and compressor stations, Bridger population data is always used for these strata.

Table 1. Sampled and population counts across strata for the EIA-based definition of the Haynesville Basin.

Stratum	Fraction of Surveyed Emitting	Survey Facility Counts	Bridger Population Count	Fraction Sampled
Marginal Producing Well Facilities	30%	1,090	22,834	5%
Standard Producing Well Facilities	37%	275	4,317	6%
High Producing Well Facilities	62%	289	1,250	23%
Compressor Stations	78%	176	274	64%
Gas Processing Plants	71%	131	168	78%
Non-Producing	43%	218	1,476	15%
No Equipment*	NA	204	NA	NA
TOTAL	**39%**	**2,383**	**30,319**	**8%**

*Facilities labeled "no equipment" are those included in sample planning that were found to have no equipment when surveyed.

The sample was drawn using stratified random sampling. Using past measurements from the Haynesville Basin to estimate the within-strata emission rate variability, a Neyman allocation was used to determine stratum sample sizes. This method prioritizes sampling strata whose emissions

distributions have the largest variance. Although operator, age, state, and production method were not explicitly used as stratification variables during the sampling process, we conducted post-sampling checks to ensure representativeness. These checks included direct comparisons of the sample and population distributions for production levels and facility age, as well as spatial distribution assessments using heatmaps.

Bridger executed the survey design and collected ~2,500 facility scans across ~2,400 unique facilities during a five-week campaign over the Haynesville basin in late summer 2024. About 34% of these scans indicated emissions. This includes ~100 scans that are repeat measurements at facilities and another ~100 for which an emission source was detected, but the rate could not be quantified. These measurements cover 8% of all facilities in the Haynesville basin based on Bridger population estimates. Source-level Bridger emissions data were filtered to a snapshot emissions distribution (i.e., first fly over) and then aggregated to the facility-level to produce a facility-level emission rate distribution. The dataset was then anonymized by Bridger to ensure that individual emission events cannot be externally traced back to specific facilities or operators. This anonymization resulted in a facility-level dataset without georeference that identified the facility strata and, if present, the total site emissions.

2.3. Extrapolation

Extrapolation is needed to create a comprehensive annual, basin level emissions inventory, as available measurements cover only a subset of facilities at a snapshot in time and are likely to have missed very small emissions sources. The methods used to perform these extrapolations are briefly described here, as they were derived from those published previously[30] and are further described in SI Section S1. While extrapolation allows us to obtain an annual basin level emissions inventory estimate, this estimate is based on only instantaneous measurements from a subset of facilities collected over less than one month. An assumption underlying the methods here is that the average

emission rate across multiple facilities in a stratum at a snapshot in time is representative of the time-averaged, facility-normalized emissions for the entire population in that stratum.[53] This inherently implies the stationarity of emission rate distributions (i.e., emission profiles of ensembles of facilities are consistent over time). We extrapolate first to account for small undetected emissions, then temporally extrapolate, and then spatially extrapolate.

We account for small undetected emissions in the Bridger survey using published emissions data and a Bayesian analysis approach. We rely on the emission rate distribution from production facilities reported by Omara et al.[7,51] to characterize small undetected emissions. Omara et al. synthesized over 1,500 site-level production sector emissions estimates across 8 production basins in the U.S. from numerous studies relying on highly sensitive technologies, such as the Environmental Protection Agency's (EPA) Other Test Method 33A, which can detect and measure lower emission rates than Bridger, including some quantified emission rates < 0.1 kg/h. To better represent Haynesville, we filter this dataset to the 1,163 facilities in dry gas basins, including the Marcellus, Fayetteville, and Barnett basins. If emissions were detected at a facility, we assume all emissions were captured. Emissions imputation is limited to the three production strata—high-producing, standard-producing, and marginal-producing well facilities—since we are not aware of any emissions distributions in the literature for the other facility types from a more sensitive technology. All non-detects in the non-production strata are treated as non-emitting in the analysis.

We use a full detection limit from the Bridger campaign and a Bayesian imputation approach to infer emissions below the full detection limit. We define the full detection limit as the emission rate at which Bridger's published POD curve indicates a 99% probability of detection, given the average wind speed and raster gas concentration noise during the 2024 Haynesville Basin campaign.[45] This calculated threshold is 1.6 kg/h, and we assume that any emission above this

threshold was detected. We assume the Omara et al.[7,51] distribution reasonably represents our data so that we can use it to estimate the percentage of sites with undetected emissions. For those sites we apply a Bayesian approach that utilizes Bridger's POD function and a log-normal parametric fit to the filtered Omara et al. data to assign the small non-zero emission rates. This process is described in more detail in SI section S1.

Facility-level emissions are temporally and spatially extrapolated according to Equations 1 and 2. The temporal extrapolation constituted multiplying the measured emission rate in per hour units by the number of hours per year. This results in an unbiased estimate of total emissions for the sampled units within each stratum and is mathematically equivalent to estimating the average emission rate for each stratum and scaling that average by the number of sampled facilities. Emissions are spatially extrapolated to include non-sampled facilities by scaling the temporally extrapolated total for a strata by the inverse of the fraction sampled in that strata, separately for each stratum. The uncertainties calculated for this work are based on a bootstrap analysis with 100,000 iterations that accounts only for the uncertainty associated with the emissions sampling and extrapolation. Measurement uncertainty is not incorporated here because algorithms to estimate Bridger's measurement uncertainty had not yet been fully developed at the time of measurement.[54]

$$Annual\ Facility\ Emissions\ (AFE) = Mean\ Measured\ Emission\ Rate \times 8760 \quad \text{Eq. 1}$$

$$Annual\ Total\ Emissions = \sum_{all\ strata}\left(AFE_{strata} \times \frac{N\ sites_{strata}}{N\ measured\ sites_{strata}}\right) \quad \text{Eq. 2}$$

2.4. CH_4 Intensity Calculation

Part of the ambiguity in CH_4 intensity stems from how production is defined. *Natural gas gross withdrawals* (i.e., produced) are defined by the EIA as the total well-stream volume of produced natural gas, excluding condensate, whereas *marketed natural gas* (i.e., marketed) excludes all

natural gas vented, flared, reinjected, or used as fuel on facility.[55] Importantly, this means emissions are included in the numerator and denominator of CH_4 intensity when using produced gas. Note both values still include condensates, liquids, and nonhydrocarbon gases removed from the gas stream during processing. While neither value is inappropriate, they will result in different CH_4 intensities, and therefore any ambiguity in which is used can lead to misinterpretation or inappropriate comparison of CH_4 intensities. Additionally, production datasets may only provide one measure of production. We present two commonly used calculation methods in this work, using both produced and marketed gas for each, for a total of four methods. More thorough discussions of the various methods are available in recent articles.[33,36]

First, we calculate what was termed in Johnson et al.[36] as a Methane Intensity that represents the true loss rate (MI_{LR}) , as shown in Equation 3. MI_{LR} represents the percentage of produced or marketed natural gas emitted. The initial analysis uses the MI_{LR} with produced gas. We assume the gas composition is 90% CH_4, as discussed as a national average in Alvarez et al.[3] and specific for the Haynesville Basin in Peischl et al.[56,57] based on United States Geological Survey data. Formally,

$$MI_{LR} = \frac{CH_4\ Emissions_{volume}}{CH_4\ content\ of\ natural\ gas_{volume}}\ . \qquad \text{Eq. 3}$$

The Oil and Gas Climate Initiative (OGCI) defines a second common CH_4 intensity, which is used by many operators targeting the 0.2% CH_4 intensity goal stated in OGMP 2.0.[34] According to the OGCI framework,[34] this CH_4 intensity is defined as shown in Equation 4, which was termed in Johnson et al.[36] as a Methane to Whole Gas Ratio (MGR_{WG}). We calculate MGR_{WG} for secondary analyses,

$$MGR_{WG} = \frac{CH_4\ Emissions_{volume}}{natural\ gas_{volume}}. \qquad \text{Eq. 4}$$

All relevant conversion factors and example calculations are provided in SI Section S3. There are several additional CH_4 intensity calculation methods not shown here that have been discussed in recent research, some of which can be easily interconverted between, while others represent distinct quantities.[33,36] While no method is incorrect, they are not all directly comparable and may appear more favorable in different conditions. As discussed in Seymour et al.,[33] the MGR_{WG} for a basin with natural gas that is 50% CH_4 would be half as much as it would be if the denominator were the methane content rather than whole gas, making it difficult to compare across basins. As recommended by some reporting programs like the Natural Gas Sustainability Initiative,[13] we also account for mixed O&G production when calculating the CH_4 intensity. This involves weighting emissions by the fraction of total energy produced from natural gas. As the Haynesville Basin is a dry gas basin, this is a minimal adjustment. According to Enverus production data, only 0.86% and 0.02% of energy produced in the Haynesville Basin comes from oil for the EIA-based and Enverus basin definitions, respectively, though this type of correction can have a significant impact for production regions with both oil and natural gas production.

3. Results and Discussion

3.1. Emission Inventory and Intensity

For the initial analysis, the comprehensive emissions inventory estimate for the Haynesville Basin is 760 [610, 940] Gg/year (95% confidence interval). Imputed emission rates below the Bridger full detection limit account for 0.3% of this total. This fraction is smaller than estimates from studies that scale facility emissions to basin emissions using similar methods, but this may be due to the large variability across basins. Thorpe et al.[48] estimated imputed emissions of 5% in the Permian Basin and 15% in the Eagle Ford Basin using Bridger data, while Sherwin et al.[37] estimated imputed emissions from 5% to over 85% across multiple basins with an instrument

283 focused on larger emissions than that used in this work (i.e., a system that would have more
284 imputed emissions).

285 We provide the average emissions per stratum and the fraction of the basin's total emissions from
286 each stratum in SI Section S2. Bridger detected emissions on 34% of their scans across all facilities
287 and the average emission rate at facilities with emissions was 28 kg/h. As has been reported
288 previously, we see an increase in emissions with increasing production.[49–51,58] The average
289 estimated emissions and the fraction of basin-total emissions for each stratum in this study also
290 show good agreement with Williams et al.[59] and Chen et al.[60]

291 Recent research has shown evidence of diurnal and seasonal patterns in emissions from oil and
292 gas production.[61–63] If these findings are representative of the sector then common assumptions
293 used when extrapolating measurement data will need to be reconsidered as the understanding
294 progresses for the entire field. More frequent measurements can be used to capture this seasonal
295 cycle in emissions so it could be accounted for directly when extrapolating, once the data and
296 understanding advance for the field. This could be done at the facility scale or using regional
297 satellite estimates of the seasonal cycle for incorporation into extrapolation methods.[61,62] Point
298 sensor network or tall tower regional measurements of diurnal patterns could similarly be
299 incorporated.[63] Additional data on the persistence of these patterns over time and how they may
300 vary regionally or across asset types (e.g., upstream as opposed to midstream) is suggested for
301 future research.

302 Our Haynesville Basin estimate, as well as those from previous studies that have focused on the
303 Haynesville Basin for comparison, are provided in Figure 2. This production data is from Enverus,
304 though the exact spatial extent may vary between studies as values provided in the literature are
305 used. This study's emissions inventory is higher than previously reported values, though within

uncertainties. Importantly, all estimates in Figure 2, other than those from Shen et al.[64], represent snapshot measurements. Schwietzke et al.[65] showed that basin total emissions estimates from the Fayetteville Basin varied by over 20% on consecutive flight days, demonstrating the potential variability in emission estimates over time. The Haynesville Basin has generally increased production over time as shown in Figure 2B and research has often shown a weak positive correlation between production and emissions.[5,29,37,48,50]

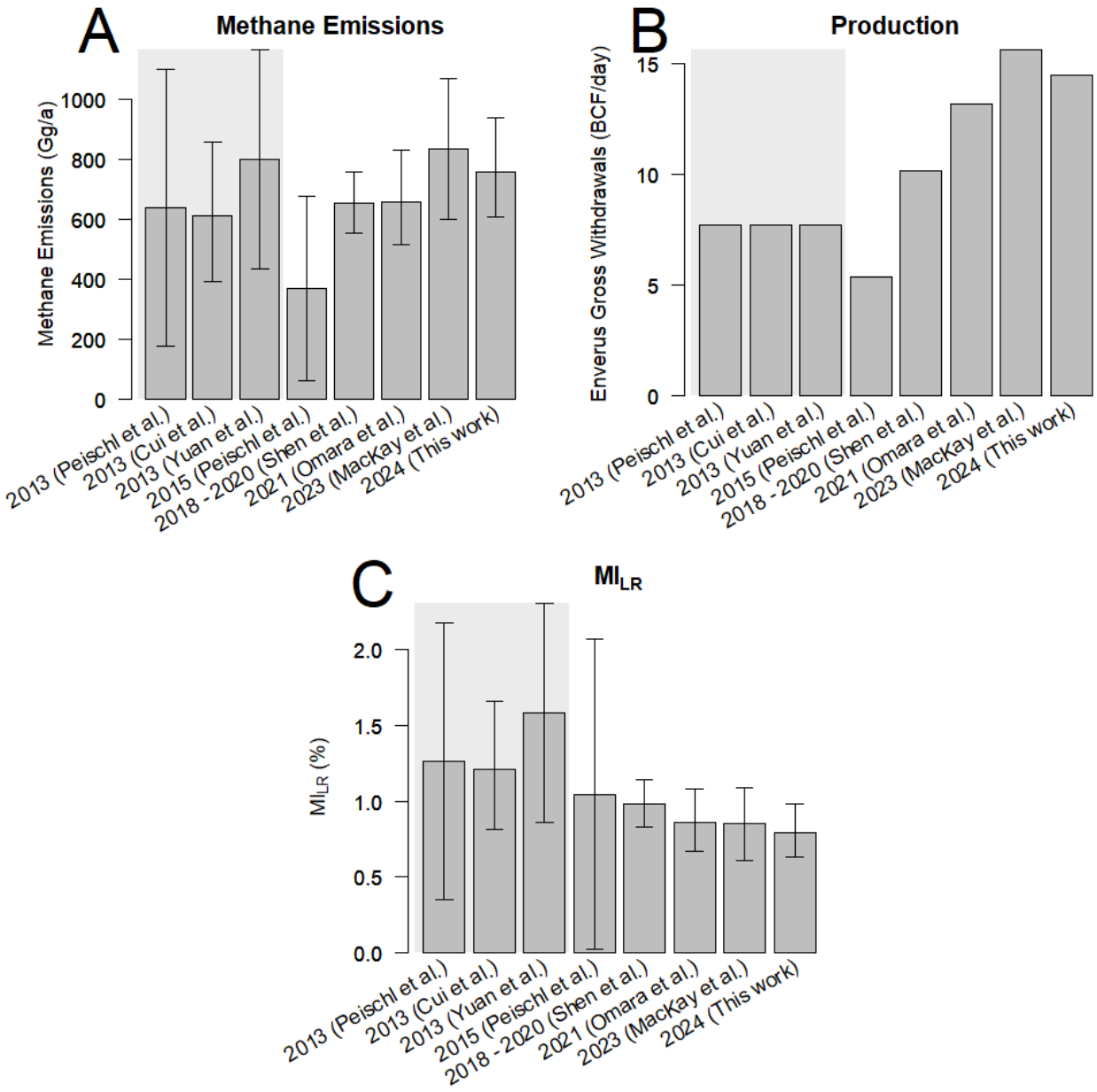

Figure 2. A) Emissions, B) production, and C) MI_{LR} values for the Haynesville Basin across several studies, all relying on Enverus production data.[7,41,56,57,64,66–68] The studies with a grey background are all based on the same measurement data using different emission rate estimation methods. See SI Table S9 for details concerning these studies.

318 CH_4 intensity is a more useful metric than emissions for comparing across regions, basins, and
319 years because it normalizes by production and can account for co-produced oil.[33,36] Figure 2C
320 shows that while this work estimates a higher CH_4 emission inventory than most previous works,
321 the MI_{LR} of 0.79% [0.63%, 0.98%] is in line with previous estimates. Note that some of the
322 presented values[56,57,68] were calculated for a measured subset of the Haynesville Basin (> 85%),
323 and researchers have shown that MI_{LR} can vary significantly at the sub-basin scale.[37,65]
324 Figure 3 provides relevant estimates of MI_{LR} from the literature across basins. As researchers
325 generally find that more productive and drier basins have lower MI_{LR},[50,51,69] we only compare the
326 estimates from this study to reported values from similar dry gas basins and national estimates.
327 We present only studies that include clear details of the MI_{LR} calculation, including production
328 data, to ensure an appropriate comparison. These values are provided solely as context for the
329 Haynesville Basin MI_{LR} estimate presented in this work, as previous works have more thoroughly
330 compared estimates across basins.[3,37,57,58,70]
331

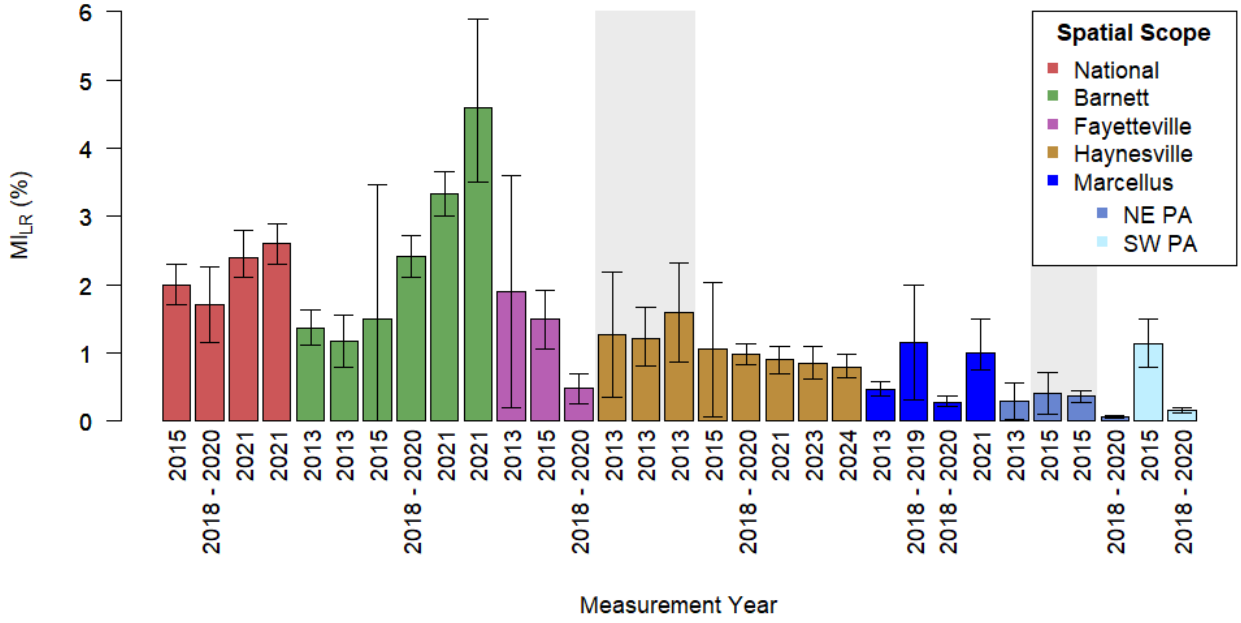

Figure 3. Reported MI_{LR} values across studies using a variety of emissions estimation methods for the U.S.[3,7,58,64] and for U.S. dry gas basins, including the Barnett,[6,7,35,37,57,64] Fayetteville,[56,64,65] Haynesville,[7,56,57,64,66–68] and Marcellus.[7,37,64,67,70–72] Some studies focused on only northeastern (NE) or southwestern (SW) Pennsylvania (PA), given the large extent of the Marcellus Basin. Studies grouped together in grey backgrounds are based on the same measurement data using different methods. The CH_4 composition used across studies ranges from 80% to 97%. See SI Table S9 for details concerning these studies.

3.2. Impact of Methodological Variations

Methodological choices for estimating emissions and emissions intensity can have notable impacts on the resulting estimates, as demonstrated in this section. The sampling method for this study used Bridger facility count estimates and the EIA-based definition of the Haynesville Basin. The initial analysis was performed utilizing this information. The secondary analyses presented in this section illustrate the impact some methodological choices can have on analysis results. Note that the comparisons we make in this section are used to illustrate how methodological choices

affect the resulting emissions intensities derived from the same underlying measurement data but would be inappropriate in practice. These comparisons illustrate the risks associated with disregarding, or not transparently disclosing, the methods with a reported CH_4 intensity, making it difficult to avoid such inappropriate comparisons over time or across basins.

Table 2 presents the results from all variations mentioned in Section 2. The most notable discrepancy is between the Enverus and EIA-based definitions of the Haynesville Basin. As described in Section 2.1, the EIA-based definition is an 18-county outline, while Enverus assigns the basin for all wells using a combination of Enverus-defined shapefiles and the likely geological formation.

Table 2. CH_4 emissions, natural gas production, and CH_4 intensity across variations considered. The initial analysis is in bold font.

Basin Definition	**EIA-based**		**Enverus**
Facility Population Data	**Bridger***	**Enverus**	**Enverus**
CH_4 emissions (Gg/year)	**760 [610, 940]**	700 [560, 860]	430 [350, 520]
Enverus produced gas (BCF/d)	**14.45**	14.45	13.45
EIA marketed gas (BCF/d)	12.35	12.35	NA$
MI_{LR} from produced gas	**0.79 [0.63, 0.98]**	0.73 [0.59, 0.90]	0.49 [0.39, 0.59]
MGR_{WG} from produced gas	0.71 [0.57, 0.85]	0.66 [0.53, 0.81]	0.44 [0.35, 0.53]
MI_{LR} from marketed gas	0.93 [0.74, 1.11]	0.85 [0.69, 1.05]	NA$
MGR_{WG} from marketed gas	0.83 [0.67, 1.03]	0.77 [0.62, 0.95]	NA$

*Bridger population counts were only provided based on the EIA-based definition of the basin
$EIA marketed production is only available for the EIA-based definition of the basin

First, we can consider the last two columns, which both use Enverus facility population data, differing only in the definition of the basin. This changes the emissions, as the population used to extrapolate emissions and the breakdown by strata change, as detailed in SI Table S2. As it includes far fewer facilities, the emission inventory based on the Enverus definition of the Haynesville Basin is 39% smaller than that based on the EIA-based definition. However, as the number of high and standard producing wells is reduced far less than that of marginal wells, the total production is only reduced by 7%. As such, the MI_{LR} is 34% smaller than what was reported when using the same Enverus facility population data, but the EIA-based definition of the Haynesville Basin. This stresses the significant impact of spatial scope for CH_4 intensity, as has been noted in some recent literature.[37,73] While both approaches might be used to characterize emissions, the estimates represent somewhat different areas and sets of facilities. Without careful qualification, both spatial extents could reasonably be referred to as the Haynesville Basin, despite their differences.

Secondly, we can compare the first two data columns, which both rely on the EIA-based basin definition but different facility population data. Switching from Bridger to Enverus facility population data results in an ~8% reduction in calculated emissions and MI_{LR} compared to the initial analysis. This has a much smaller impact than changing basin definition as changing the population data reduces the well site counts by ~23% while changing the basin definition reduces the well site counts by ~70%. Additionally, when changing population data, some strata counts increase while others decrease. Changing the basin definition causes all strata counts to decrease, particularly marginal producing well sites. Table S2 in the SI provides all population count estimates. It is important to note that we are using the same population data for non-production strata across all variations, given Enverus only provides well counts. Therefore, the difference between the emission estimates and MI_{LR} is solely due to changes in production facility counts.

We can consider this an uncertainty estimate in the underlying facility population data, though additional datasets exist that may differ from both of those used here (e.g., operator records, state datasets).

Thirdly, we can see the impact of using produced or marketed natural gas. The MI_{LR} from the initial analysis is 0.79 [0.63, 0.98] % and the MI_{LR} marketed for the same column is 0.93 [0.74, 1.11] %, a 17% increase. This difference is due to the annual produced natural gas metric from Enverus (14.45 BCF/day) being 17% larger than the EIA marketed amount (12.35 BCF/day). However, the difference between these is variable over time and across basins. Looking at June 2013, the timeframe of Peischl et al.,[56] gross withdrawals in the Haynesville Basin according to Enverus[41] (7.4 BCF/day) and EIA[39] (7.9 BCF/day) were about 48% larger than marketed natural gas, according to the EIA[39] (5.2 BCF/day). This changes their MI_{LR} from 1.26 [0.35, 2.18] using produced gas to 1.87 [0.52, 3.23] % using marketed.

Lastly, we can see the impact of accounting for the gas composition by comparing MI_{LR} to MGR_{WG}. The initial analysis resulted in a MI_{LR} of 0.79 [0.63, 0.98] % as compared to an MGR_{WG} for the same column of 0.71 [0.57, 0.85] %, a 10% reduction. MI_{LR} is calculated using the lower volume of methane produced rather than the volume of natural gas produced. For the Haynesville, we use a composition of 90% CH_4,[3,56,57] but it is important to stress that this composition can also vary regionally and over time. Peischl et al.[57] showed that the CH_4 content of the natural gas produced in six regions ranged from 47% to 90% based on previously published literature and United States Geological Survey data. As discussed in Seymour et al.,[33] this means there are regions with a 50% CH_4 composition that would see a 50% reduction in the estimated CH_4 intensity due solely to this effect.

406 ## 3.3. Implications

407 This study highlights important decision points that can influence a calculated CH_4 intensity.
408 The selection of statistical extrapolation methods for estimating annual basin-scale emissions from
409 snapshots was discussed in previous work.[30] Therefore, we focus on the definition of the basin, the
410 source of population infrastructure information, and the method used to calculate the denominator
411 of the intensity. While it is not always clear how to define each of these CH_4 intensity calculation
412 inputs, each of them has the potential to meaningfully impact the result. For example, in this study,
413 changing the basin definition led to a large change in CH_4 intensity, whereas uncertainty in the
414 facility population had a small impact. The combined impacts of methodological changes
415 considered in this work changed the estimated CH_4 intensity from 0.93% for the MI_{LR} using
416 marketed gas with Bridger data for the EIA basin definition to 0.44% for the MGR_{WG} using
417 produced gas with Enverus data for the Enverus basin definition. We have also provided examples
418 to discuss that many of the methodological decisions varied in this work can result in more
419 substantial differences than seen here. Though some of these methodological decisions have been
420 discussed individually in other works, this is the first study examining the combined effect these
421 inputs can have at the basin scale.

422 Critically, none of these differences make a value incorrect, but each CH_4 intensity represents
423 something slightly different and is therefore not directly comparable, despite the fact that each CH_4
424 intensity in Table 2 can reasonably be described as a Haynesville Basin CH_4 intensity estimate.
425 Appropriately considering this is critical both for benchmarking an operator's intensity within a
426 basin relative to the basin as a whole and to making meaningful comparisons of results across
427 basins or time. Ultimately, this work highlights some of the complexities that need to be
428 considered in incentives and regulations based on CH_4 intensity, such as those suggested by the
429 EU.[18]

There is no clear justification for recommending specific methodological choices from this work. The impact these choices have on the calculated CH_4 intensity emphasizes the importance of more transparency and methodological detail whenever discussing a CH_4 intensity. As each entity (e.g., operator, regulator, researcher) that calculates a methane intensity may have different goals and limitations (e.g., lack of access to commercial databases), we do not believe a single pathway is necessarily the best approach to addressing this concern. To ensure the repeatability, comparability, and value of the CH_4 intensity metric, we recommend transparently providing methodological detail. We provide a list of key information necessary to properly understand, compare, and calculate a CH_4 intensity in Table 3. This builds on recent work that walked through the process of reconciling divergent emission and CH_4 intensity estimates between two O&G studies.[73] They detailed the impact of differences in instrumentation, measurement, and processing methods. Additional recent works have also discussed the importance of providing the details underlying the CH_4 intensity calculation method, stressing such information can enable conversion from one method to another for some cases and certain calculation methods.[33,36] Our recommendation is that information listed in Table 3 should always be clearly provided when presenting a CH_4 intensity estimate. This information can also be incorporated into voluntary reporting frameworks and regulations that would use CH_4 intensity to compare across operators/basins. If these details are provided, then CH_4 intensities can be better understood such that any methodological differences can be accounted for as much as possible to improve the comparability and value of the CH_4 intensity metric.

451 **Table 3.** Aspects of a CH_4 intensity calculation that must be provided to ensure transparency,
452 repeatability, and comparability.

Attribute	Description
Time period	Temporal boundary for emissions and production (e.g., annual)
Spatial scope	Spatial boundary for emissions and production
	Facilities or natural gas industry segment (i.e., upstream, midstream) covered
Data sources	Datasets used for production and, if used, facility population (e.g., EIA, Enverus)
CH_4 intensity calculation method	The production with clear units
	The estimated emissions with clear units
	The method used to account for oil, if applied
	The type of production data (i.e., produced, marketed)
	Equation used with clear units (e.g., natural gas, CH_4 content of natural gas, Joules)
	Any other relevant variables used in the calculation (CH_4 fraction, CH_4 density, heating values, etc.)
Emissions measurement technology and estimation method	Relevant methods used to estimate emissions inventory from measurements (e.g., extrapolation methods used to scale facility measurements to basin total)
	Relevant instrument performance metrics such as POD
	Measurement/survey approach

453

454 Notes

455 The authors declare no competing financial interest.

456 Supporting Information

457 The following files are available free of charge.

458 A full list of the counties used to define the Haynesville Basin using the EIA-based definition
459 (Table S1); Population data for the Haynesville Basin across variations considered (Table S2);
460 Probabilities used to impute emissions for marginal, standard, and high production facilities
461 (Tables S3 – S5); Average emissions by strata (Table S6); Proportion of basin total emissions from
462 each strata (Table S7); Oil and gas production for both basin definitions (Table S8); Details of the
463 literature referenced in Figures 2 and 3 (Table S9); Detailed description of the extrapolation
464 method used to account for undetected emissions (Text S1); Emissions by strata and comparison
465 to literature (Text S2); Detailed description of how CH_4 intensity is calculated, including examples
466 (Text S3); Probability distribution functions used to impute emissions (Figure S1 – S3) (PDF).

467 Anonymized data and processing code used in this work is available at
468 (https://github.com/yroell-gti/haynesvillebasin_mii_extrapolations).

469 Abbreviations

470 O&G, oil and gas; U.S., United States; CH_4, methane; CO_2, carbon dioxide; OGMP, Oil and Gas
471 Methane Partnership; EU, European Union; MII, measurement-informed inventory; EIA, Energy
472 Information Administration; BCF, billion cubic feet; SI, Supporting Information; GML, Gas
473 Mapping LiDAR; POD, probability of detection; BOED, Barrels of Oil Equivalent per Day;
474 EPA, Environmental Protection Agency; OGCI, oil and gas climate initiative; MI_{LR}, methane
475 intensity true loss rate; MGR_{WG}, methane to whole gas ratio

476 Acknowledgements

477 This work was funded by the U.S. Department of Energy (Agreement DE-FE0032298), the GTI
478 Energy Center for Methane Research, and GTI Energy.

References

(1) U.S. EPA. *Inventory of U.S. Greenhouse Gas Emissions and Sinks: 1990-2022*; Reports and Assessments; 2024. https://www.epa.gov/ghgemissions/inventory-us-greenhouse-gas-emissions-and-sinks-1990-2022 (accessed 2025-05-19).

(2) Forster, P.; Storelvmo, T.; Armour, K.; Collins, W.; Dufresne, J.-L.; Frame, D.; Lunt, D. J.; Mauritsen, T.; Palmer, M. D.; Watanabe, M.; et al. The Earth's Energy Budget, Climate Feedbacks, and Climate Sensitivity. In *Climate Change 2021: The Physical Science Basis. Contribution of Working Group I to the Sixth Assessment Report of the Intergovernmental Panel on Climate Change*; Masson-Delmotte, V., Zhai, P., Pirani, A., Connors, S. L., Péan, C., Berger, S., Caud, N., Chen, Y., Goldfarb, L., Gomis, M. I., et al., Eds.; Cambridge University Press, Cambridge, United Kingdom and New York, NY, USA, 2021; pp 923–1054.

(3) Alvarez, R. A.; Zavala-Araiza, D.; Lyon, D. R.; Allen, D. T.; Barkley, Z. R.; Brandt, A. R.; Davis, K. J.; Herndon, S. C.; Jacob, D. J.; Karion, A.; et al. Assessment of Methane Emissions from the U.S. Oil and Gas Supply Chain. *Science* **2018**, *361* (6398), 186–188. https://doi.org/10.1126/science.aar7204.

(4) Brandt, A. R.; Heath, G. A.; Kort, E. A.; O'Sullivan, F.; Pétron, G.; Jordaan, S. M.; Tans, P.; Wilcox, J.; Gopstein, A. M.; Arent, D.; et al. Methane Leaks from North American Natural Gas Systems. *Science* **2014**, *343* (6172), 733–735. https://doi.org/10.1126/science.1247045.

(5) Johnson, M. R.; Conrad, B. M.; Tyner, D. R. Creating Measurement-Based Oil and Gas Sector Methane Inventories Using Source-Resolved Aerial Surveys. *Commun. Earth Environ.* **2023**, *4* (1), 1–9. https://doi.org/10.1038/s43247-023-00769-7.

(6) Lyon, D. R.; Zavala-Araiza, D.; Alvarez, R. A.; Harriss, R.; Palacios, V.; Lan, X.; Talbot, R.; Lavoie, T.; Shepson, P.; Yacovitch, T. I.; et al. Constructing a Spatially Resolved Methane Emission Inventory for the Barnett Shale Region. *Environ. Sci. Technol.* **2015**, *49* (13), 8147–8157. https://doi.org/10.1021/es506359c.

(7) Omara, M.; Himmelberger, A.; MacKay, K.; Williams, J. P.; Benmergui, J.; Sargent, M.; Wofsy, S. C.; Gautam, R. Constructing a Measurement-Based Spatially Explicit Inventory of US Oil and Gas Methane Emissions (2021). *Earth Syst. Sci. Data* **2024**, *16* (9), 3973–3991. https://doi.org/10.5194/essd-16-3973-2024.

(8) *The Oil and Gas Emissions Management Regulations*; 2019; Vol. Reg 7. https://www.saskatchewan.ca/business/agriculture-natural-resources-and-industry/oil-and-gas/environmental-protection/oil-and-gas-emissions-management (accessed 2025-06-18).

(9) *Consolidated Federal Laws of Canada, Regulations Respecting Reduction in the Release of Methane and Certain Volatile Organic Compounds (Upstream Oil and Gas Sector)*; 2023; Vol. 2018–66. https://laws-lois.justice.gc.ca/eng/regulations/SOR-2018-66/ (accessed 2025-06-18).

(10) Electronic Code of Federal Regulations. *40 Code of Federal Regulations §60.5360b - 60.5439b*; 2024. https://www.ecfr.gov/current/title-40/part-60/subpart-OOOOb (accessed 2025-06-18).

(11) *Global Decarbonization Charter at COP28*. UN Climate Summit News - COP29. https://unclimatesummit.org/cop28-explainers-2/global-decarbonization-charter-at-cop28/ (accessed 2025-06-18).

(12) *Global Methane Tracker 2024 – Analysis*. IEA. https://www.iea.org/reports/global-methane-tracker-2024 (accessed 2025-06-18).

(13) Natural Gas Sustainability Initiative (NGSI). *Natural Gas Sustainability Initiative (NGSI)*. American Gas Association. https://www.aga.org/research-policy/natural-gas-esg-sustainability/natural-gas-sustainability-initiative-ngsi/ (accessed 2025-05-30).
(14) Oil and Gas Climate Initiative. *Learn about Reducing methane emissions - OGCI*. Oil and Gas Climate Initiative. https://www.ogci.com/methane-emissions/methane-intensity-target (accessed 2025-05-29).
(15) ONE Future. *ONE Future is a coalition of natural gas companies working collaboratively to reduce methane emissions across the value chain through innovative technologies and shared best practices.* https://onefuture.us/ (accessed 2025-05-21).
(16) GTI Energy. *Veritas*. https://veritas.gti.energy/ (accessed 2025-04-09).
(17) MiQ. *MiQ is the fastest growing and most trusted methane emissions certification standard*. https://miq.org/ (accessed 2025-04-09).
(18) EUR-Lex. *Regulation (EU) 2024/1787 of the European Parliament and of the Council of 13 June 2024 on the Reduction of Methane Emissions in the Energy Sector and Amending Regulation (EU) 2019/942 (Text with EEA Relevance)*; 2024. http://data.europa.eu/eli/reg/2024/1787/oj/eng (accessed 2025-05-22).
(19) Littlefield, J.; Rai, S.; Skone, T. J. Life Cycle GHG Perspective on U.S. Natural Gas Delivery Pathways. *Environ. Sci. Technol.* **2022**, *56* (22), 16033–16042. https://doi.org/10.1021/acs.est.2c01205.
(20) Roman-White, S.; Rai, S.; Littlefield, J.; Cooney, G.; Skone, T. J. *Life Cycle Greenhouse Gas Perspective on Exporting Liquefied Natural Gas from the Unites States: 2019 Update*; DOE/NETL-2019/2041; National Energy Technology Laboratory (NETL), Pittsburgh, PA, Morgantown, WV, and Albany, OR (United States), 2019. https://doi.org/10.2172/1607677.
(21) The Inner City Fund. *Lifecycle GHG Emissions of US LNG Exports*; 2024. https://naturalalliesforcleanenergy.org/wp-content/uploads/2024/07/NACEF-LNG-Exports.pdf (accessed 2025-05-22).
(22) Howarth, R. W. The Greenhouse Gas Footprint of Liquefied Natural Gas (LNG) Exported from the United States. *Energy Sci. Eng.* **2024**, *12* (11), 4843–4859. https://doi.org/10.1002/ese3.1934.
(23) United Nations Environment Programme. *The Oil & Gas Methane Partnership 2.0*. https://www.ogmpartnership.org/ (accessed 2024-12-20).
(24) Kleinberg, R. L. Problems with Greenhouse Gas Life Cycle Analyses of U.S. LNG Exports and Locally Produced Coal. EarthArXiv April 1, 2024. https://doi.org/10.31223/X5C98Z.
(25) The White House. *FACT SHEET: Biden-Harris Administration Announces Temporary Pause on Pending Approvals of Liquefied Natural Gas Exports*. The White House. https://bidenwhitehouse.archives.gov/briefing-room/statements-releases/2024/01/26/fact-sheet-biden-harris-administration-announces-temporary-pause-on-pending-approvals-of-liquefied-natural-gas-exports/ (accessed 2025-05-22).
(26) Schissel, C.; Allen, D.; Dieter, H. Methods for Spatial Extrapolation of Methane Measurements in Constructing Regional Estimates from Sample Populations. *Environ. Sci. Technol.* **2024**, *58* (6), 2739–2749. https://doi.org/10.1021/acs.est.3c08185.
(27) Schissel, C.; Allen, D. T. Impact of the High-Emission Event Duration and Sampling Frequency on the Uncertainty in Emission Estimates. *Environ. Sci. Technol. Lett.* **2022**, *9* (12), 1063–1067. https://doi.org/10.1021/acs.estlett.2c00731.
(28) Conrad, B. M.; Tyner, D. R.; Li, H. Z.; Xie, D.; Johnson, M. R. A Measurement-Based Upstream Oil and Gas Methane Inventory for Alberta, Canada Reveals Higher Emissions and

Different Sources than Official Estimates. *Commun. Earth Environ.* **2023**, *4* (1), 1–10. https://doi.org/10.1038/s43247-023-01081-0.

(29) Wang, J. L.; Daniels, W. S.; Hammerling, D. M.; Harrison, M.; Burmaster, K.; George, F. C.; Ravikumar, A. P. Multiscale Methane Measurements at Oil and Gas Facilities Reveal Necessary Frameworks for Improved Emissions Accounting. *Environ. Sci. Technol.* **2022**, *56* (20), 14743–14752. https://doi.org/10.1021/acs.est.2c06211.

(30) Fosdick, B. K.; Weller, Z. D.; Wong, H. X.; Corbett, A.; Roell, Y.; Martinez, E.; Berry, A.; Gielczowski, N.; Hajny, K. D.; Moore, C. Extrapolation Approaches for Creating Comprehensive Measurement-Based Methane Emissions Inventories. *ACS EST Air* **2026**, *3* (3), 862–874. https://doi.org/10.1021/acsestair.5c00455.

(31) Zavala-Araiza, D.; Alvarez, R. A.; Lyon, D. R.; Allen, D. T.; Marchese, A. J.; Zimmerle, D. J.; Hamburg, S. P. Super-Emitters in Natural Gas Infrastructure Are Caused by Abnormal Process Conditions. *Nat. Commun.* **2017**, *8* (1), 14012. https://doi.org/10.1038/ncomms14012.

(32) Zavala-Araiza, D.; Lyon, D. R.; Alvarez, R. A.; Davis, K. J.; Harriss, R.; Herndon, S. C.; Karion, A.; Kort, E. A.; Lamb, B. K.; Lan, X.; et al. Reconciling Divergent Estimates of Oil and Gas Methane Emissions. *Proc. Natl. Acad. Sci.* **2015**, *112* (51), 15597–15602. https://doi.org/10.1073/pnas.1522126112.

(33) Seymour, S.; Xie, D.; Kang, M.; Schwietzke, S.; Zavala-Araiza, D.; Hamburg, S. Methane Emission Intensity Metrics: Unmasking the Trade-Offs. Research Square May 28, 2025. https://doi.org/10.21203/rs.3.rs-6753363/v1.

(34) Oil and Gas Climate Initiative. *Oil & Gas Climate Initiative Reporting Framework | OGCI Methane Library*. https://methanelibrary.ogci.com/resource/oil-gas-climate-initiative-reporting-framework/ (accessed 2025-06-02).

(35) Karion, A.; Sweeney, C.; Kort, E. A.; Shepson, P. B.; Brewer, A.; Cambaliza, M.; Conley, S. A.; Davis, K.; Deng, A.; Hardesty, M.; et al. Aircraft-Based Estimate of Total Methane Emissions from the Barnett Shale Region. *Environ. Sci. Technol.* **2015**, *49* (13), 8124–8131. https://doi.org/10.1021/acs.est.5b00217.

(36) Johnson, M. R.; Conrad, B. M.; Zimmerle, D. J.; Kleinberg, R. L. Methane by the Numbers: The Need for Clear and Comparable Methane Intensity Metrics. *Environ. Sci. Technol.* **2026**, *60* (11), 8258–8265. https://doi.org/10.1021/acs.est.5c13990.

(37) Sherwin, E. D.; Rutherford, J. S.; Zhang, Z.; Chen, Y.; Wetherley, E. B.; Yakovlev, P. V.; Berman, E. S. F.; Jones, B. B.; Cusworth, D. H.; Thorpe, A. K.; et al. US Oil and Gas System Emissions from Nearly One Million Aerial Site Measurements. *Nature* **2024**, *627* (8003), 328–334. https://doi.org/10.1038/s41586-024-07117-5.

(38) *Waste Emissions Charge for Petroleum and Natural Gas Systems: Procedures for Facilitating Compliance, Including Netting and Exemptions*; 2024; Vol. 2024–26643, pp 91094–91195. https://www.federalregister.gov/documents/2024/11/18/2024-26643/waste-emissions-charge-for-petroleum-and-natural-gas-systems-procedures-for-facilitating-compliance (accessed 2025-06-18).

(39) U.S. EIA. Short-Term Energy Outlook. https://www.eia.gov/outlooks/steo/data.php (accessed 2026-02-11).

(40) U.S. EIA. *Oil and Gas County Code Master List - Energy Information Administration*. https://www.eia.gov/naturalgas/fieldcode/ (accessed 2025-05-29).

(41) Enverus. Enverus PRISM Energy Analytics. https://www.enverus.com/solutions/energy-analytics/ep/prism/ (accessed 2026-02-05).

(42) Esri; TomTom; Garmin; FAO; NOAA; USGS; OpenStreetMap(c) contributors; the GIS User Community. 2025.
(43) Bell, C. S.; Rutherford, J.; Brandt, A.; Sherwin, E.; Vaughn, T.; Zimmerle, D. Single-Blind Determination of Methane Detection Limits and Quantification Accuracy Using Aircraft-Based LiDAR. *Elem. Sci. Anthr.* **2022**, *10* (1), 00080. https://doi.org/10.1525/elementa.2022.00080.
(44) Conrad, B. M.; Tyner, D. R.; Johnson, M. R. Robust Probabilities of Detection and Quantification Uncertainty for Aerial Methane Detection: Examples for Three Airborne Technologies. *Remote Sens. Environ.* **2023**, *288*, 113499. https://doi.org/10.1016/j.rse.2023.113499.
(45) Thorpe, M. J.; Kreitinger, A.; Altamura, D. T.; Dudiak, C. D.; Conrad, B. M.; Tyner, D. R.; Johnson, M. R.; Brasseur, J. K.; Roos, P. A.; Kunkel, W. M.; et al. Deployment-Invariant Probability of Detection Characterization for Aerial LiDAR Methane Detection. *Remote Sens. Environ.* **2024**, *315*, 114435. https://doi.org/10.1016/j.rse.2024.114435.
(46) Thorpe, M. J.; Donahue, C. P.; Kreitinger, A.; Roos, P. A.; Brasseur, J. K.; Losby, B.; Greenfield, N.; Carre-Burritt, A.; Kunkel, W. M.; Altamura, D. T.; et al. Total Emissions Estimation for Oil and Gas Production Facilities Using Aerial Gas Mapping LiDAR; 2024; p D011S015R002. https://doi.org/10.2118/222020-MS.
(47) Gupta, S.; Tullos, E.; Lyon, D.; Ma, H.; Ravikumar, A. Evaluating Practical Detection Limits for Aerial Methane Technologies Using Large Scale Field Measurements. ChemRxiv. https://doi.org/10.26434/chemrxiv-2025-816nt.
(48) Hmiel, B.; Lyon, D. R.; Warren, J. D.; Yu, J.; Cusworth, D. H.; Duren, R. M.; Hamburg, S. P. Empirical Quantification of Methane Emission Intensity from Oil and Gas Producers in the Permian Basin. *Environ. Res. Lett.* **2023**, *18* (2), 024029. https://doi.org/10.1088/1748-9326/acb27e.
(49) Lyman, S. N.; Tran, T.; Mansfield, M. L.; Ravikumar, A. P. Aerial and Ground-Based Optical Gas Imaging Survey of Uinta Basin Oil and Gas Wells. *Elem. Sci. Anthr.* **2019**, *7*, 43. https://doi.org/10.1525/elementa.381.
(50) Lyon, D. R.; Alvarez, R. A.; Zavala-Araiza, D.; Brandt, A. R.; Jackson, R. B.; Hamburg, S. P. Aerial Surveys of Elevated Hydrocarbon Emissions from Oil and Gas Production Sites. *Environ. Sci. Technol.* **2016**, *50* (9), 4877–4886. https://doi.org/10.1021/acs.est.6b00705.
(51) Omara, M.; Zimmerman, N.; Sullivan, M. R.; Li, X.; Ellis, A.; Cesa, R.; Subramanian, R.; Presto, A. A.; Robinson, A. L. Methane Emissions from Natural Gas Production Sites in the United States: Data Synthesis and National Estimate. *Environ. Sci. Technol.* **2018**, *52* (21), 12915–12925. https://doi.org/10.1021/acs.est.8b03535.
(52) *Energy Industry Data (GIS & more)*. Rextag Corporation Store. https://rextag.com/ (accessed 2025-05-30).
(53) Pandey, S.; Worden, J.; Cusworth, D. H.; Varon, D. J.; Thill, M. D.; Jacob, D. J.; Bowman, K. W. Relating Multi-Scale Plume Detection and Area Estimates of Methane Emissions: A Theoretical and Empirical Analysis. *Environ. Sci. Technol.* **2025**, *59* (16), 7931–7947. https://doi.org/10.1021/acs.est.4c07415.
(54) Dudiak, C. D.; Goodwin, D. B.; Altamura, D.; Donahue, C. P.; Thorpe, M. Quantification Error Model for Aerial LiDAR Methane Emission Rate Estimates. EarthArXiv November 11, 2025. https://doi.org/10.31223/X5TT9J.
(55) U.S. EIA. *Glossary - U.S. Energy Information Administration (EIA)*. https://www.eia.gov/tools/glossary/index.php (accessed 2025-05-29).

(56) Peischl, J.; Ryerson, T. B.; Aikin, K. C.; de Gouw, J. A.; Gilman, J. B.; Holloway, J. S.; Lerner, B. M.; Nadkarni, R.; Neuman, J. A.; Nowak, J. B.; et al. Quantifying Atmospheric Methane Emissions from the Haynesville, Fayetteville, and Northeastern Marcellus Shale Gas Production Regions. *J. Geophys. Res. Atmospheres* **2015**, *120* (5), 2119–2139. https://doi.org/10.1002/2014JD022697.

(57) Peischl, J.; Eilerman, S. J.; Neuman, J. A.; Aikin, K. C.; de Gouw, J.; Gilman, J. B.; Herndon, S. C.; Nadkarni, R.; Trainer, M.; Warneke, C.; et al. Quantifying Methane and Ethane Emissions to the Atmosphere From Central and Western U.S. Oil and Natural Gas Production Regions. *J. Geophys. Res. Atmospheres* **2018**, *123* (14), 7725–7740. https://doi.org/10.1029/2018JD028622.

(58) Williams, J. P.; Omara, M.; Himmelberger, A.; Zavala-Araiza, D.; MacKay, K.; Benmergui, J.; Sargent, M.; Wofsy, S. C.; Hamburg, S. P.; Gautam, R. Small Emission Sources in Aggregate Disproportionately Account for a Large Majority of Total Methane Emissions from the US Oil and Gas Sector. *Atmospheric Chem. Phys.* **2025**, *25* (3), 1513–1532. https://doi.org/10.5194/acp-25-1513-2025.

(59) Omara, M.; Zavala-Araiza, D.; Lyon, D. R.; Hmiel, B.; Roberts, K. A.; Hamburg, S. P. Methane Emissions from US Low Production Oil and Natural Gas Well Sites. *Nat. Commun.* **2022**, *13* (1), 2085. https://doi.org/10.1038/s41467-022-29709-3.

(60) Chen, Y.; Sherwin, E. D.; Berman, E. S. F.; Jones, B. B.; Gordon, M. P.; Wetherley, E. B.; Kort, E. A.; Brandt, A. R. Quantifying Regional Methane Emissions in the New Mexico Permian Basin with a Comprehensive Aerial Survey. *Environ. Sci. Technol.* **2022**, *56* (7), 4317–4323. https://doi.org/10.1021/acs.est.1c06458.

(61) Hu, L.; Andrews, A. E.; Montzka, S. A.; Miller, S. M.; Bruhwiler, L.; Oh, Y.; Sweeney, C.; Miller, J. B.; McKain, K.; Ibarra Espinosa, S.; et al. An Unexpected Seasonal Cycle in U.S. Oil and Gas Methane Emissions. *Environ. Sci. Technol.* **2025**, *59* (20), 9968–9979. https://doi.org/10.1021/acs.est.4c14090.

(62) Varon, D. J.; Jacob, D. J.; Estrada, L. A.; Balasus, N.; East, J. D.; Pendergrass, D. C.; Chen, Z.; Sulprizio, M.; Omara, M.; Gautam, R.; et al. Seasonality and Declining Intensity of Methane Emissions from the Permian and Nearby US Oil and Gas Basins. *Environ. Sci. Technol.* **2026**, *60* (1), 425–435. https://doi.org/10.1021/acs.est.5c08745.

(63) Barkley, Z. R.; Davis, K. J.; Miles, N. L.; Richardson, S. J. Examining Daily Temporal Characteristics of Oil and Gas Methane Emissions in the Delaware Basin Using Continuous Tower Observations. *J. Geophys. Res. Atmospheres* **2025**, *130* (6), e2024JD042050. https://doi.org/10.1029/2024JD042050.

(64) Shen, L.; Gautam, R.; Omara, M.; Zavala-Araiza, D.; Maasakkers, J. D.; Scarpelli, T. R.; Lorente, A.; Lyon, D.; Sheng, J.; Varon, D. J.; et al. Satellite Quantification of Oil and Natural Gas Methane Emissions in the US and Canada Including Contributions from Individual Basins. *Atmospheric Chem. Phys.* **2022**, *22* (17), 11203–11215. https://doi.org/10.5194/acp-22-11203-2022.

(65) Schwietzke, S.; Pétron, G.; Conley, S.; Pickering, C.; Mielke-Maday, I.; Dlugokencky, E. J.; Tans, P. P.; Vaughn, T.; Bell, C.; Zimmerle, D.; et al. Improved Mechanistic Understanding of Natural Gas Methane Emissions from Spatially Resolved Aircraft Measurements. *Environ. Sci. Technol.* **2017**, *51* (12), 7286–7294. https://doi.org/10.1021/acs.est.7b01810.

(66) Cui, Y. Y.; Brioude, J.; McKeen, S. A.; Angevine, W. M.; Kim, S.-W.; Frost, G. J.; Ahmadov, R.; Peischl, J.; Bousserez, N.; Liu, Z.; et al. Top-down Estimate of Methane Emissions in California Using a Mesoscale Inverse Modeling Technique: The South Coast Air Basin. *J.*

Geophys. Res. Atmospheres **2015**, *120* (13), 6698–6711. https://doi.org/10.1002/2014JD023002.

(67) Yuan, B.; Kaser, L.; Karl, T.; Graus, M.; Peischl, J.; Campos, T. L.; Shertz, S.; Apel, E. C.; Hornbrook, R. S.; Hills, A.; et al. Airborne Flux Measurements of Methane and Volatile Organic Compounds over the Haynesville and Marcellus Shale Gas Production Regions. *J. Geophys. Res. Atmospheres* **2015**, *120* (12), 6271–6289. https://doi.org/10.1002/2015JD023242.

(68) MacKay, K.; Benmergui, J.; Williams, J. P.; Omara, M.; Himmelberger, A.; Sargent, M.; Warren, J. D.; Miller, C. C.; Roche, S.; Zhang, Z.; et al. Assessment of Methane Emissions from US Onshore Oil and Gas Production Using MethaneAIR Measurements. *Atmospheric Chem. Phys.* **2026**, *26* (2), 1179–1192. https://doi.org/10.5194/acp-26-1179-2026.

(69) Robertson, A. M.; Edie, R.; Snare, D.; Soltis, J.; Field, R. A.; Burkhart, M. D.; Bell, C. S.; Zimmerle, D.; Murphy, S. M. Variation in Methane Emission Rates from Well Pads in Four Oil and Gas Basins with Contrasting Production Volumes and Compositions. *Environ. Sci. Technol.* **2017**, *51* (15), 8832–8840. https://doi.org/10.1021/acs.est.7b00571.

(70) Ren, X.; Hall, D. L.; Vinciguerra, T.; Benish, S. E.; Stratton, P. R.; Ahn, D.; Hansford, J. R.; Cohen, M. D.; Sahu, S.; He, H.; et al. Methane Emissions from the Marcellus Shale in Southwestern Pennsylvania and Northern West Virginia Based on Airborne Measurements. *J. Geophys. Res. Atmospheres* **2019**, *124* (3), 1862–1878. https://doi.org/10.1029/2018JD029690.

(71) Barkley, Z. R.; Lauvaux, T.; Davis, K. J.; Deng, A.; Miles, N. L.; Richardson, S. J.; Cao, Y.; Sweeney, C.; Karion, A.; Smith, M.; et al. Quantifying Methane Emissions from Natural Gas Production in North-Eastern Pennsylvania. *Atmospheric Chem. Phys.* **2017**, *17* (22), 13941–13966. https://doi.org/10.5194/acp-17-13941-2017.

(72) Schneising, O.; Buchwitz, M.; Reuter, M.; Vanselow, S.; Bovensmann, H.; Burrows, J. P. Remote Sensing of Methane Leakage from Natural Gas and Petroleum Systems Revisited. *Atmospheric Chem. Phys.* **2020**, *20* (15), 9169–9182. https://doi.org/10.5194/acp-20-9169-2020.

(73) Chen, Y.; Sherwin, E. D.; Wetherley, E. B.; Yakovlev, P. V.; Berman, E. S. F.; Jones, B. B.; Hmiel, B.; Lyon, D. R.; Duren, R.; Cusworth, D. H.; et al. Reconciling Ultra-Emitter Detections from Two Aerial Hyperspectral Imaging Surveys in the Permian Basin. **2024**.

Supporting Information for:

Challenges with Developing a Measurement-Based Basin Methane Intensity Estimate: A Case Study from the Haynesville

*Kristian D. Hajny[1], Bailey K. Fosdick[1], Zachary Weller[1], Ella Martinez[1], Hon Xing Wong[1], Abigail Corbett[1], Christopher Moore[1, *]*

[1] GTI Energy

This document contains 21 pages with 3 text sections (Text S1-S3), 3 figures (Figure S1 – S3) and 9 tables (Table S1 – S9)

Supporting Information

Table S1. List of all counties in the EIA-based definition of the Haynesville Basin.

1	BIENVILLE, LA	7	SABINE, LA	13	NACOGDOCHES, TX
2	BOSSIER, LA	8	WEBSTER, LA	14	PANOLA, TX
3	CADDO, LA	9	ANGELINA, TX	15	RUSK, TX
4	DE SOTO, LA	10	GREGG, TX	16	SABINE, TX
5	NATCHITOCHES, LA	11	HARRISON, TX	17	SAN AUGUSTINE, TX
6	RED RIVER, LA	12	MARION, TX	18	SHELBY, TX

Table S2. Population counts across production strata for both the EIA-based and Haynesville definition of the Haynesville Basin using the Enverus and Bridger population data. Bridger population estimates were not provided for the Enverus definition of the Haynesville Basin. Enverus data includes only production sites. Given this, Bridger population counts were used for other strata even when using Enverus activity data.

Stratum	Survey Facility Counts	Bridger Population Count (EIA-based domain)	Enverus Population Count (EIA-based domain)	Enverus Population Count (Enverus domain)
Marginal Producing Well Sites	1,090	22,834	14,449	1,375
Standard Producing Well Sites	275	4,317	5,471	3,136
High Producing Well Sites	289	1,250	2,045	1,974
Compressor Stations	176	274	NA	NA
Gas Processing Plants	131	168	NA	NA
Non-Producing	218	1,476	NA	NA
No Equipment	204	NA	NA	NA
TOTAL	**1,654**	**30,319**	**21,965**	**6,485**

S1. Accounting for Emissions Below the Full Detection Limit

Our measurement-based methane emissions inventory for the Haynesville Basin was developed using two sources of methane emissions data: measurements collected by Bridger as described in main text Section 2.2, and upstream facility emissions from Omara et al.[1,2] Omara et al. synthesized methane emissions measurements from multiple studies focused on onshore, U.S. natural gas production sites. The aggregated studies used ground-based measurements to estimate methane emissions across multiple natural gas-producing basins. The ground-based measurements are from highly sensitive technologies that enable quantification of emission rates as small as 0.06 kg/hr and include Hi-Flow, downwind tracer flux, and downwind methane plume modeling.[3] Thus, we expect these data contain a greater proportion of small emission rates than collected during the Bridger aerial survey. For this analysis, we assume the Omara emissions data are the "truth" and that no emissions below Bridger's full detection limit for this specific campaign were undetected.

The Omara emissions data were filtered to include only measurements from basins with characteristics like the Haynesville Basin (e.g., dry gas). Based on feedback from our operator partners, measurements from the Marcellus, Fayetteville, and Barnett basins were kept for our analysis. This filtering resulted in 1,163 facility-level emissions measurements.

S1.1 Calculating the probabilities of a non-detect and a non-zero emission

Before conducting spatial and temporal extrapolations, we first finalized the emissions dataset to be used. This required imputing small emissions from the Omara et al. data to replace some non-detects in the Bridger data. A "non-detect" is any case where Bridger measured zero emissions. The initial step in this process was to infer Bridger's full detection limit specific to this campaign. We define the full detection limit as the emission rate at which Bridger's probability of detection (POD) curve indicates a 99% probability of detection, given the average wind speed and

raster gas concentration noise (GCN) during the campaign. For the 2024 survey, this threshold was calculated to be 1.6 kg/hr. Accordingly, we assumed that any emission above this threshold was detected, and any imputed emission must be less than or equal to 1.6 kg/hr. Note that the Bridger POD model was developed for source-level estimates, and using it at the facility level as done here assumes facilities have no sources or only one source. 46% of emitting facilities had only one source.

We assumed that some non-detects from the Bridger aerial campaign represented emissions below the full detection limit, while others were truly non-emitting sites. To estimate the proportion of each, we used relative distributions from the Omara et al. data. Specifically, we applied these proportions to the basin-level aerial data to distinguish between non-emitting facilities and those with emissions below the 1.6 kg/hr threshold. We use Table S3 focused on marginal-producing sites as an example, but the process is also applied to standard- and high-producing sites, shown in Tables S4 and S5, respectively.

In Tables S3-S5, we categorize facilities into four groups: (1) non-emitting, (2) 0-1.6 kg/hr (undetected), (3) 0-1.6 kg/hr (detected), and (4) >1.6 kg/hr (detected). For the Omara et al. data, we know the fractions of facilities that are non-emitting, have detected emissions between 0 and 1.6 kg/hr, and have detected emissions greater than 1.6 kg/hr. Since we assume that all emissions in the 0-1.6 kg/hr range are detected in the Omara et al. data, there is no category for undetected emissions in that range.

For marginal-producing facilities in the Omara et al. data, the distribution is as follows: 19% are non-emitting, 45% have detected emissions between 0 and 1.6 kg/hr, and 36% have detected emissions >1.6 kg/hr. In contrast, the Bridger aerial data provides the following distribution for marginal-producing facilities: 75% are either non-emitting or have undetected emissions below

817 1.6 kg/hr, 11% have detected emissions between 0 and 1.6 kg/hr, and 14% have detected emissions
818 >1.6 kg/hr.

819 To align the ratio of facilities with emissions between 0 and 1.6 kg/hr (detected or undetected)
820 to those with emissions greater than 1.6 kg/hr between the two datasets, we apply a scaling factor.
821 Specifically, we multiply the 14% of Bridger facilities with >1.6 kg/hr emissions by the ratio of
822 45% to 36% from the Omara et al. data. This yields an adjusted estimate of 17.5% of Bridger data
823 facilities with emissions between 0 and 1.6 kg/hr (detected or undetected). Subtracting the known
824 11% with detected emissions in this range gives 6.5% as the estimated proportion with undetected
825 emissions. Finally, subtracting this 6.5% from the combined 75% of non-emitting and undetected
826 facilities yields an estimated 68.5% of facilities that are truly non-emitting in the Bridger data.

827 The estimated probabilities that a non-detect corresponds to either a truly non-emitting facility
828 or one with non-zero emissions below 1.6 kg/hr are derived from the proportions calculated earlier.
829 For marginal-producing facilities, the probability that a non-detect is truly non-emitting is 0.91.
830 This is calculated by dividing the estimated proportion of non-emitting facilities (68.5%) by the
831 total proportion of facilities that are either non-emitting or have undetected emissions below 1.6
832 kg/hr (75%). Consequently, the probability that a non-detect is a facility with non-zero emissions
833 below 1.6 kg/hr is 0.09 (i.e., 1 – 0.91). This same approach is applied to standard- and high-
834 producing facilities. It is important to note that this approach was not used for the compressor
835 station and gas processing plant strata due to differences in emissions characteristics between
836 midstream and upstream facilities. The proportion of facilities in these two strata with emissions
837 greater than the 1.6 kg/hr threshold was so large that the method outlined above failed, resulting
838 in a negative proportion of emissions allocated to non-emitting facilities. This suggests the

emission distribution of the Omara et al. production site dataset differs too significantly from our measured emissions distribution from these sites.

S1.2 Using Bayes' Theorem to impute non-zero emissions

Having estimated the probabilities of a non-detect corresponding to a truly non-emitting facility ($p = 0.91$) or a non-zero emission below 1.6 kg/hr ($p = 0.09$), the next step is to impute the missing emission rates. For this we leverage Bayes' Theorem, listed in Equation S1, which allows us to calculate the probability distribution of emission rates given no emissions were detected. The prior distribution, denoted P(emission rate), is derived from a parametric fit to the Omara et al. data. This prior distribution is multiplied by the likelihood of a non-detection as a function of the emission rate, based on Bridger's POD and is denoted P(non-detect | emission rate). The resulting normalized posterior distribution, denoted P(emission rate | non-detect), is the conditional distribution of emission rates given it was a non-detect. Equation S1 specifies this conditional distribution, assuming a finite set of possible emission rates below the full detection limit for simplicity. We sample from this posterior distribution to impute emission rates for non-detects. Here we are using the Bridger POD model for facility-level when it is designed for the facility-level. Doing so assumes that facilities have no more than one source, which was only true for 46% of emitting facilities in this dataset.

If a non-zero emission rate in the range (0, 1.6) is to be generated, the specific value is assigned according to a probability function which is the convolution of two elements: Bridger's probability of non-detection function, defined as one minus Bridger's POD function,[4] and a parametric probability function fit to the Omara et al.[1,2] emissions data within the range of 0 to 1.6 kg/hr. The first component gives a higher probability that non-detections are smaller emissions since these are more likely to be missed in an aerial survey and the second component represents the expected emission distribution for those less than 1.6 kg/hr, reflecting the frequency at which emissions of

863 various sizes are seen on production sites. Aligning with Bayes' Theorem, we multiplied Bridger's
864 probability of non-detection function by the parametric probability density function fit to the
865 Omara et al. data, then normalized. All functions were defined in the range from 0.01 kg/h to 1.6
866 kg/h in 0.01 kg/h increments. The final probability function is plotted in SI Figure S3.

867 The imputation process is quite simple once all of the necessary probabilities and probability
868 functions are computed. For each marginal-producing non-detect, the process begins with a binary
869 determination of the emission rate: there is a 91% probability that the assigned rate will be 0 kg/h,
870 and a 9% probability that a non-zero rate will be assigned. If a non-zero rate is selected, a value is
871 then sampled from the pre-defined probability function described above, where possible values
872 range from 0.01 kg/h to 1.6 kg/h in 0.01 kg/h increments, each weighted according to the given
873 probability distribution. Each facility non-detection is generated independently, ensuring that
874 outcomes for one facility do not affect future emission rate assignments.

875 $$P(emission \mid non-detect|) = \frac{P(non-detect|emission|)P(emission)}{P(non-detect)}$$ Eq. S1

876 **Table S3.** Table providing estimated fraction of marginal-producing facilities in different
877 emissions rate categories for the Omara and basin-level aerial data.

	Omara	Basin-Level Aerial Data	
Non-emitting	26.6%	75.0%	**64.7%****
0 - 1.6 kg/h (undetected)	N/A		**10.3%***
0 - 1.6 kg/h (detected)	44.5%	11.1%	
>1.6 kg/h (detected)	28.9%	13.9%	

878 * **10.3%** = 13.9% * (44.5% / 28.9%) - 11.1%; ** **64.7%** = 75.0% - 10.3%

879

880

Table S4. Table providing estimated fraction of standard-producing facilities in different emissions rate categories for the Omara and basin-level aerial data.

	Omara	Basin-Level Aerial Data	
Non-emitting	15.3%	67.3%	**40.5%****
0 - 1.6 kg/h (undetected)	N/A		**26.8%***
0 - 1.6 kg/h (detected)	54.4%	11.4%	
>1.6 kg/h (detected)	30.3%	21.3%	

* **26.8%** = 21.3% * (54.4% / 30.3%) - 11.4%; ** **40.5%** = 67.3% - 26.8%

Table S5. Table providing estimated fraction of high-producing facilities in different emissions rate categories for the Omara and basin-level aerial data.

	Omara	Basin-Level Aerial Data	
Non-emitting	19.3%	40.2%	**22.5%****
0 - 1.6 kg/h (undetected)	N/A		**17.7%***
0 - 1.6 kg/h (detected)	35.8%	16.7%	
>1.6 kg/h (detected)	44.9%	43.1%	

* **17.7%** = 43.1% * (35.8% / 44.9%) - 16.7%; ** **22.5%** = 40.2% - 17.7%

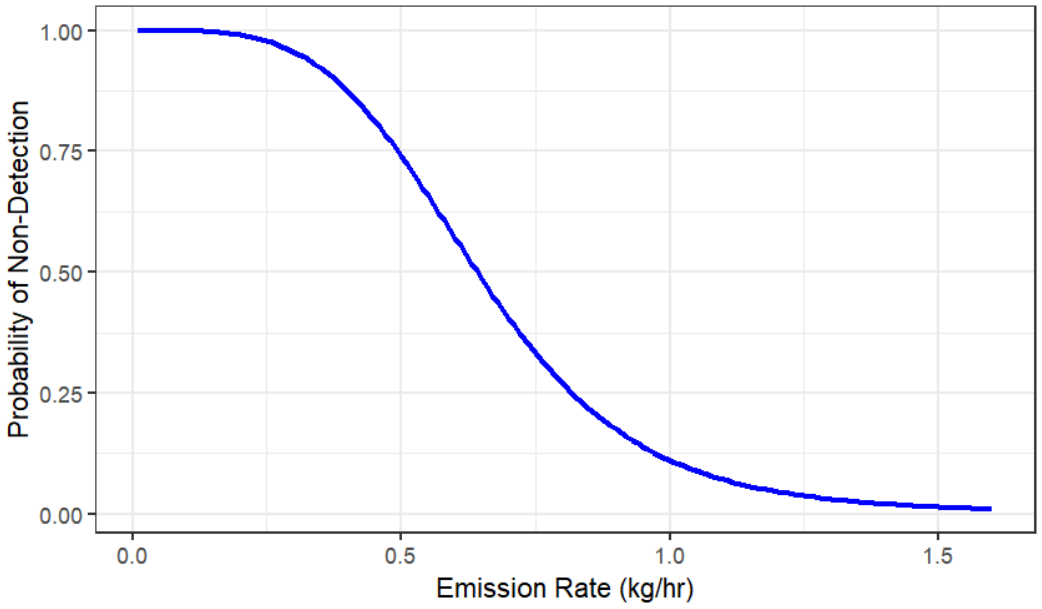

Figure S1: Bridger's probability of non-detection, computed as one minus the probability of detection. The Bridger POD model was developed for source level estimates and using it at the

facility level as done here assumes facilities have no sources or only one source, which was the case for 46% of emitting facilities.

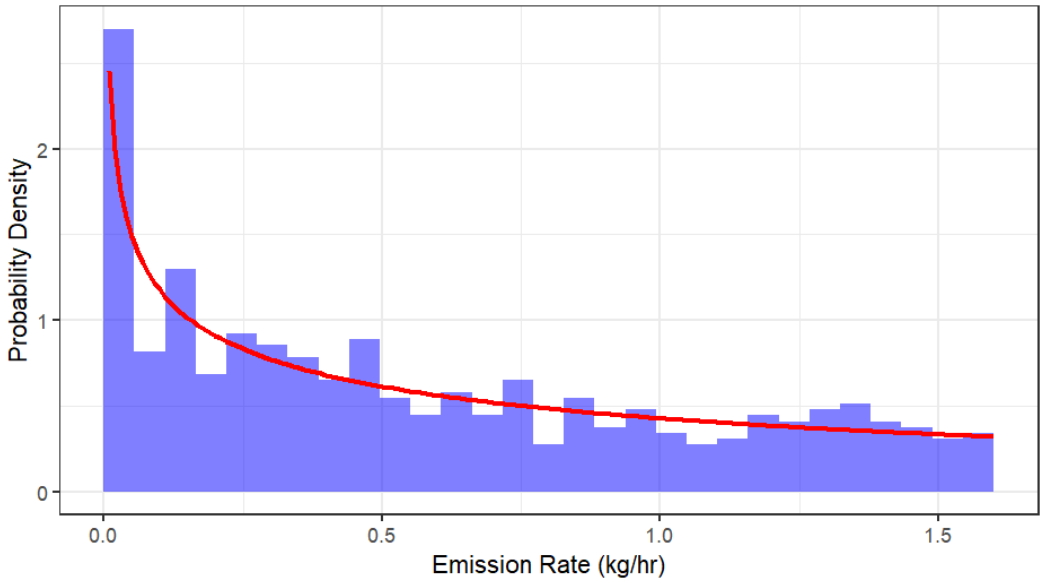

Figure S2: A parametric probability density function (PDF) (red line) fit to the Omara et al. emissions data < 1.6 kg/h (blue histogram).

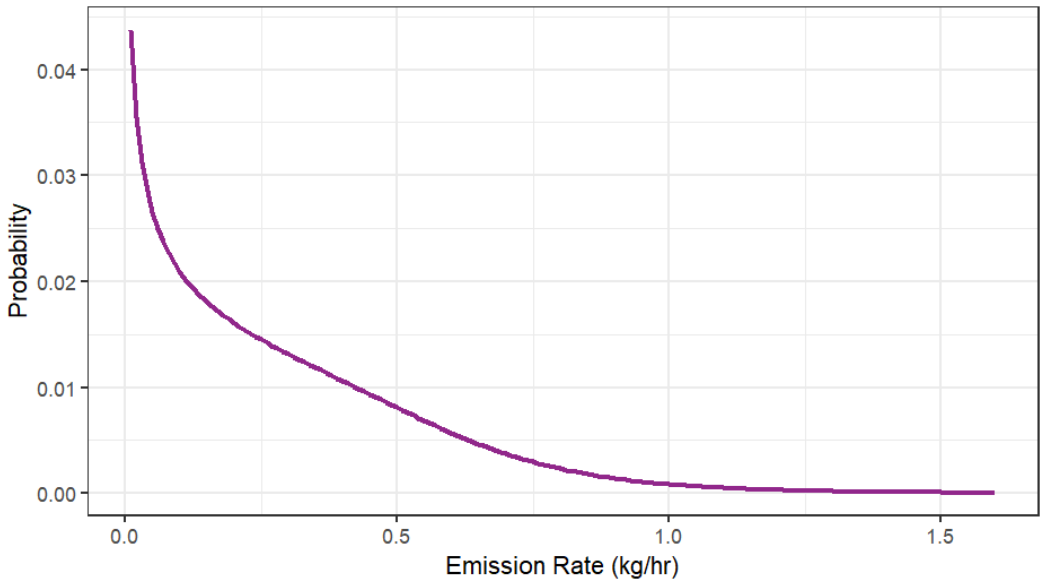

Figure S3. Probability function derived from Bridger's POD and a parametric fit to the Omara et al. data.

901

S2. Emissions by Facility Type

Table S6 presents the average emissions by strata. The average emissions for most strata calculated in this study also agree well with Williams et al.,[5] who simulated national emissions using a large suite of previously published facility-level measurement data. The most significant difference is that the average emission rate from gas processing plants measured in this study is considerably lower.

Table S6. Average emissions by strata including zeros for this and previous works in kg/h.

Stratum	This work	Williams et al.[6]
Production-standard and high (> 15 BOED)	3.8 [2.5, 5.6]	3.3 [2.9, 3.8]
Production-marginal (0 – 15 BOED)	1.3 [1.0, 1.8]	1.3 [1.2, 1.5]
Compressor stations	50.4 [32.2, 72.1]	52 [47, 60]
Gas processing plants	73.2 [50.6, 99.3]	146 [115, 283]
Other	7.5 [2.2, 16.9]	NA

We also see general agreement with previous works regarding the relative contribution of different strata to the basin inventory, as presented in Table S7. Table S7 shows the fraction of facilities in each stratum for the region being considered, as different basins may have a different mix of facility types. Chen et al.[7] used similar aerial surveys to measure emissions from the New Mexican Permian Basin. This work shows a similar fraction of total emissions from production facilities compared to these previous studies. The fraction of production emissions from marginal wells in this work (58%) is also in good agreement with Williams et al.[6] (65%) and Omara et al.[5] (54% [37%, 75%]). This means that a large fraction of total emissions from production facilities

come from marginal wells producing little natural gas. However, Table S6 and Table S7 also show that such wells have smaller emissions per facility. They represent a large fraction of total emissions as the overwhelming majority (75%) of production facilities are marginal wells.

Table S7. The fraction of basin-total emissions and basin-total facility counts by strata for this and previous work. The relative counts provided for this work are based on the Bridger population counts from Table 1. The percentages of basin-total emissions for this work are based on these Bridger population counts scaled by mean emission rates from the Bridger measurement campaign.

Stratum	**This work**	**Chen et al.**[7]	**Williams et al.**[6]
Measurement year	2024	2018 – 2020	2021
Basin	Haynesville	New Mexican Permian	National
Production-non-marginal well facilities	24% (18% of facilities)	52% (57% of facilities)	24% (18% of facilities)
Production-marginal well facilities	34% (75% of facilities)		44% (80% of facilities)
Compressor station	16% (1% of facilities)	17% (12% of facilities)	20% (1% of facilities)
Gas processing plant	14% (1% of facilities)	2% (2% of facilities)	8% (< 1% of facilities)
Other	13% (5% of facilities)	29% (30% of facilities)	4% (< 1% of facilities)

S3. Methane Intensity Calculation

We use a CH_4 density of 0.000714 MT / m^3 at 0°C and 1 atmosphere as listed in the OGCI reporting framework[8] to convert between volume and mass of methane emissions. To convert produced natural gas to CH_4 we assume the composition of the gas is 90% CH_4, as discussed as a national average in Alvarez et al.[9] and specific for the Haynesville Basin in Peischl et al.[10,11] based on United States Geological Survey data. However, it is important to consider that the composition of natural gas varies significantly regionally and can vary over time so the appropriate value for the study area should be used.[12,13] Equations S2 – S4 provide the calculations used to convert emissions and production data to like units for the initial analysis. The MI_{LR} marketed would then be the result of Equation S2 over that of Equation S3 while the MI_{LR} produced would be the result of Equation S2 over that of Equation S4. To calculate the corresponding MGR_{WG} values the 0.9 composition term in Equations S3 and S4 is excluded.

$$\frac{756.9\ Gg\ CH_4\ emissions}{year} \times \frac{10^9 g}{Gg} \times \frac{MT}{10^6 g} \times \frac{m^3}{0.000714 MT} = \quad \text{Eq. S2}$$

$$1.06 \times 10^9\ m^3\ of\ CH_4\ emitted/year$$

$$\frac{12.35\ marketed\ natural\ gas\ BCF}{d} \times \frac{365 d}{year} \times \frac{10^9 cf}{BCF} \times \frac{0.028 m^3}{cf} \times \frac{0.9\ CH_4}{natural\ gas} = \quad \text{Eq. S3}$$

$$1.14 \times 10^{11}\ m^3\ marketed\ natural\ gas/year$$

$$\frac{14.45\ gross\ withdrawals\ of\ natural\ gas\ BCF}{d} \times \frac{365 d}{year} \times \frac{10^9 cf}{BCF} \times \frac{0.028 m^3}{cf} \times \frac{0.9\ CH_4}{natural\ gas} = \quad \text{Eq. S4}$$

$$1.33 \times 10^{11}\ m^3\ of\ CH_4\ produced\ from\ gross\ withdrawals/year$$

Lastly, we use the combined gas and oil production provided by Enverus in thousand cubic feet equivalent (MCFE) and gas production in MCF to calculate the fraction of energy produced from gas in the Haynesville Basin. As MCFE is calculated by converting all oil to its energy equivalent volume of gas, the ratio of gas in MCF to gas and oil in MCFE is equivalent to the ratio of gas in

joules (J) to gas and oil in J. The methane emission estimate, or equivalently the CH_4 intensity, is scaled by this gas to oil fraction. These fractions according to Enverus for the Haynesville Basin are provided in Table S8.

Table S8. The produced gas, combined oil and gas, and the resulting gas fraction of produced energy for the Haynesville Basin.

	EIA-based basin definition	**Enverus basin definition**
Natural gas (MCF)	5.275×10^9	4.910×10^9
Combined (MCFE)	5.321×10^9	4.911×10^9
Gas Fraction (%)	99.14	99.98

957 **Table S9.** Details regarding references used to create Figures 2 and 3.

Publication	Measurement Year	Method	CH_4 Content	Basin(s)	Comments
Alvarez et al.[9]	2015	Bottom up synthesizing many facility level measurements	90	National	
Barkley et al.[14]	2015	Regional airborne inversion optimizing intensity & regional airborne mass balance	95	NE PA	Both inversion and mass balance estimates are used
Cui et al.[15]	2013	Regional airborne inversion	90	Haynesville	Relies on the same measurements as Peischl et al.[10] and Yuan et al.[16] Emissions were converted to MI_{LR} by subtracting the non-O&G emissions provided in Peischl et al.[10] and using the production values provided in Alvarez et al.[9] for Peischl et al.[10]
Karion et al.[17]	2013	Regional airborne mass balance	89	Barnett	Using values provided in Alvarez et al.[9]

958

959

960 **Table S7 Cont.**

Lyon et al.[18]	2013	Bottom up synthesizing many facility level measurements	89	Barnett	Natural gas distribution emissions were removed
MacKay et al.[19]	2023	Airborne remote sensing area measurements	86	Haynesville	While other basins were measured, they were excluded as the percent of oil and gas activity measured was < 90%.
Omara et al.[2]	2021	Bottom up method synthesizing facility level measurements and detailed infrastructure data	80	National, Barnett, Haynesville, Marcellus	
Peischl et al.[10]	2013	Regional airborne mass balance	97 (Fayetteville) 90 (Haynesville) 95 (NE PA)	Fayetteville, Haynesville, NE PA, W Arkoma	Relies on the same measurements as Yuan et al.[16] and Cui et al.[15] Using the values provided in Alvarez et al.[9]
Peischl et al.[11]	2015	Regional airborne mass balance	87 (Barnett) 90 (Haynesville)	Bakken, Barnett, Denver-Julesburg, Eagle Ford, Haynesville	Haynesville production values were checked against Enverus to ensure gross rather than marketed values were used and they agreed within 1%

961
962

963 **Table S7 Cont.**

Ren et al.[20]	2015	Regional airborne mass balance	88	SW PA	
Schwietzke et al.[21]	2015	Regional airborne mass balance	92	Fayetteville	
Schneising et al.[22]	2018 – 2019	TROPOMI inversion	93	Marcellus	The intensity was recalculated without accounting for co-produced oil, though this has little effect given oil was only ~2% of all energy produced
Shen et al.[23]	2018 – 2020	TROPOMI inversion	90	National – including values for individual basins	Emissions and production values were converted to $MI_{LR,}$ though this may not be an appropriate composition for some basins

964

965

966 **Table S7 Cont.**

Sherwin et al.[24]	2021	Airborne remote sensing facility measurements extrapolated to the Basin level	90	Barnett, Denver-Julesburg, Marcellus, Permian, San Joaquin, Uinta	We do not include the reported Marcellus estimate as the paper states it did not sample the region comprehensively enough to appropriately scale to a basin total
Yuan et al.[16]	2013	Regional airborne eddy covariance	90 (Haynesville) 95 (Marcellus)	Haynesville, Marcellus	Relies on the same measurements as Peischl et al.[10] and Cui et al.[15] for the Haynesville. Emissions were converted to MI_{LR} by subtracting the non-O&G emissions provided in Peischl et al.[10] and using the production values provided in Alvarez et al.[9] for Peischl et al.[10]
Williams et al.[6]	2021	Bottom up synthesizing many facility level measurements	80	National	

967

References

(1) Omara, M.; Zimmerman, N.; Sullivan, M. R.; Li, X.; Ellis, A.; Cesa, R.; Subramanian, R.; Presto, A. A.; Robinson, A. L. Methane Emissions from Natural Gas Production Sites in the United States: Data Synthesis and National Estimate. *Environ. Sci. Technol.* **2018**, *52* (21), 12915–12925. https://doi.org/10.1021/acs.est.8b03535.

(2) Omara, M.; Himmelberger, A.; MacKay, K.; Williams, J. P.; Benmergui, J.; Sargent, M.; Wofsy, S. C.; Gautam, R. Constructing a Measurement-Based Spatially Explicit Inventory of US Oil and Gas Methane Emissions (2021). *Earth System Science Data* **2024**, *16* (9), 3973–3991. https://doi.org/10.5194/essd-16-3973-2024.

(3) Riddick, S. N.; Mbua, M.; Riddick, J. C.; Houlihan, C.; Hodshire, A. L.; Zimmerle, D. J. Uncertainty Quantification of Methods Used to Measure Methane Emissions of 1 g CH4 H−1. *Sensors* **2023**, *23* (22), 9246. https://doi.org/10.3390/s23229246.

(4) Thorpe, M. J.; Kreitinger, A.; Altamura, D. T.; Dudiak, C. D.; Conrad, B. M.; Tyner, D. R.; Johnson, M. R.; Brasseur, J. K.; Roos, P. A.; Kunkel, W. M.; et al. Deployment-Invariant Probability of Detection Characterization for Aerial LiDAR Methane Detection. *Remote Sensing of Environment* **2024**, *315*, 114435. https://doi.org/10.1016/j.rse.2024.114435.

(5) Omara, M.; Zavala-Araiza, D.; Lyon, D. R.; Hmiel, B.; Roberts, K. A.; Hamburg, S. P. Methane Emissions from US Low Production Oil and Natural Gas Well Sites. *Nat Commun* **2022**, *13* (1), 2085. https://doi.org/10.1038/s41467-022-29709-3.

(6) Williams, J. P.; Omara, M.; Himmelberger, A.; Zavala-Araiza, D.; MacKay, K.; Benmergui, J.; Sargent, M.; Wofsy, S. C.; Hamburg, S. P.; Gautam, R. Small Emission Sources in Aggregate Disproportionately Account for a Large Majority of Total Methane Emissions from the US Oil and Gas Sector. *Atmospheric Chemistry and Physics* **2025**, *25* (3), 1513–1532. https://doi.org/10.5194/acp-25-1513-2025.

(7) Chen, Y.; Sherwin, E. D.; Berman, E. S. F.; Jones, B. B.; Gordon, M. P.; Wetherley, E. B.; Kort, E. A.; Brandt, A. R. Quantifying Regional Methane Emissions in the New Mexico Permian Basin with a Comprehensive Aerial Survey. *Environ. Sci. Technol.* **2022**, *56* (7), 4317–4323. https://doi.org/10.1021/acs.est.1c06458.

(8) Oil and Gas Climate Initiative. *Oil & Gas Climate Initiative Reporting Framework | OGCI Methane Library*. https://methanelibrary.ogci.com/resource/oil-gas-climate-initiative-reporting-framework/ (accessed 2025-06-02).

(9) Alvarez, R. A.; Zavala-Araiza, D.; Lyon, D. R.; Allen, D. T.; Barkley, Z. R.; Brandt, A. R.; Davis, K. J.; Herndon, S. C.; Jacob, D. J.; Karion, A.; et al. Assessment of Methane Emissions from the U.S. Oil and Gas Supply Chain. *Science* **2018**, *361* (6398), 186–188. https://doi.org/10.1126/science.aar7204.

(10) Peischl, J.; Ryerson, T. B.; Aikin, K. C.; de Gouw, J. A.; Gilman, J. B.; Holloway, J. S.; Lerner, B. M.; Nadkarni, R.; Neuman, J. A.; Nowak, J. B.; et al. Quantifying Atmospheric Methane Emissions from the Haynesville, Fayetteville, and Northeastern Marcellus Shale Gas Production Regions. *Journal of Geophysical Research: Atmospheres* **2015**, *120* (5), 2119–2139. https://doi.org/10.1002/2014JD022697.

(11) Peischl, J.; Eilerman, S. J.; Neuman, J. A.; Aikin, K. C.; de Gouw, J.; Gilman, J. B.; Herndon, S. C.; Nadkarni, R.; Trainer, M.; Warneke, C.; et al. Quantifying Methane and Ethane Emissions to the Atmosphere From Central and Western U.S. Oil and Natural Gas Production Regions. *Journal of Geophysical Research: Atmospheres* **2018**, *123* (14), 7725–7740. https://doi.org/10.1029/2018JD028622.

(12) Brennan, S. T.; Rivera, J. L.; Varela, B.; Park, A. J.; Agyepong, L. A. Natural Gas Compositional Analyses Dataset of Gases from United States Wells, 2021. https://doi.org/10.5066/P9TR93E3.

(13) Zhang, T.; Sun, X.; Milliken, K. L.; Ruppel, S. C.; Enriquez, D. Empirical Relationship between Gas Composition and Thermal Maturity in Eagle Ford Shale, South Texas. *AAPG Bulletin* **2017**, *101* (8), 1277–1307. https://doi.org/10.1306/09221615209.

(14) Barkley, Z. R.; Lauvaux, T.; Davis, K. J.; Deng, A.; Miles, N. L.; Richardson, S. J.; Cao, Y.; Sweeney, C.; Karion, A.; Smith, M.; et al. Quantifying Methane Emissions from Natural Gas Production in North-Eastern Pennsylvania. *Atmospheric Chemistry and Physics* **2017**, *17* (22), 13941–13966. https://doi.org/10.5194/acp-17-13941-2017.

(15) Cui, Y. Y.; Brioude, J.; McKeen, S. A.; Angevine, W. M.; Kim, S.-W.; Frost, G. J.; Ahmadov, R.; Peischl, J.; Bousserez, N.; Liu, Z.; et al. Top-down Estimate of Methane Emissions in California Using a Mesoscale Inverse Modeling Technique: The South Coast Air Basin. *Journal of Geophysical Research: Atmospheres* **2015**, *120* (13), 6698–6711. https://doi.org/10.1002/2014JD023002.

(16) Yuan, B.; Kaser, L.; Karl, T.; Graus, M.; Peischl, J.; Campos, T. L.; Shertz, S.; Apel, E. C.; Hornbrook, R. S.; Hills, A.; et al. Airborne Flux Measurements of Methane and Volatile Organic Compounds over the Haynesville and Marcellus Shale Gas Production Regions. *Journal of Geophysical Research: Atmospheres* **2015**, *120* (12), 6271–6289. https://doi.org/10.1002/2015JD023242.

(17) Karion, A.; Sweeney, C.; Kort, E. A.; Shepson, P. B.; Brewer, A.; Cambaliza, M.; Conley, S. A.; Davis, K.; Deng, A.; Hardesty, M.; et al. Aircraft-Based Estimate of Total Methane Emissions from the Barnett Shale Region. *Environ. Sci. Technol.* **2015**, *49* (13), 8124–8131. https://doi.org/10.1021/acs.est.5b00217.

(18) Lyon, D. R.; Zavala-Araiza, D.; Alvarez, R. A.; Harriss, R.; Palacios, V.; Lan, X.; Talbot, R.; Lavoie, T.; Shepson, P.; Yacovitch, T. I.; et al. Constructing a Spatially Resolved Methane Emission Inventory for the Barnett Shale Region. *Environ. Sci. Technol.* **2015**, *49* (13), 8147–8157. https://doi.org/10.1021/es506359c.

(19) MacKay, K.; Benmergui, J.; Williams, J. P.; Omara, M.; Himmelberger, A.; Sargent, M.; Warren, J. D.; Miller, C. C.; Roche, S.; Zhang, Z.; et al. Assessment of Methane Emissions from US Onshore Oil and Gas Production Using MethaneAIR Measurements. *Atmospheric Chemistry and Physics* **2026**, *26* (2), 1179–1192. https://doi.org/10.5194/acp-26-1179-2026.

(20) Ren, X.; Hall, D. L.; Vinciguerra, T.; Benish, S. E.; Stratton, P. R.; Ahn, D.; Hansford, J. R.; Cohen, M. D.; Sahu, S.; He, H.; et al. Methane Emissions from the Marcellus Shale in Southwestern Pennsylvania and Northern West Virginia Based on Airborne Measurements. *Journal of Geophysical Research: Atmospheres* **2019**, *124* (3), 1862–1878. https://doi.org/10.1029/2018JD029690.

(21) Schwietzke, S.; Pétron, G.; Conley, S.; Pickering, C.; Mielke-Maday, I.; Dlugokencky, E. J.; Tans, P. P.; Vaughn, T.; Bell, C.; Zimmerle, D.; et al. Improved Mechanistic Understanding of Natural Gas Methane Emissions from Spatially Resolved Aircraft Measurements. *Environ. Sci. Technol.* **2017**, *51* (12), 7286–7294. https://doi.org/10.1021/acs.est.7b01810.

(22) Schneising, O.; Buchwitz, M.; Reuter, M.; Vanselow, S.; Bovensmann, H.; Burrows, J. P. Remote Sensing of Methane Leakage from Natural Gas and Petroleum Systems Revisited. *Atmospheric Chemistry and Physics* **2020**, *20* (15), 9169–9182. https://doi.org/10.5194/acp-20-9169-2020.

(23) Shen, L.; Gautam, R.; Omara, M.; Zavala-Araiza, D.; Maasakkers, J. D.; Scarpelli, T. R.; Lorente, A.; Lyon, D.; Sheng, J.; Varon, D. J.; et al. Satellite Quantification of Oil and Natural Gas Methane Emissions in the US and Canada Including Contributions from Individual Basins. *Atmospheric Chemistry and Physics* **2022**, *22* (17), 11203–11215. https://doi.org/10.5194/acp-22-11203-2022.

(24) Sherwin, E. D.; Rutherford, J. S.; Zhang, Z.; Chen, Y.; Wetherley, E. B.; Yakovlev, P. V.; Berman, E. S. F.; Jones, B. B.; Cusworth, D. H.; Thorpe, A. K.; et al. US Oil and Gas System Emissions from Nearly One Million Aerial Site Measurements. *Nature* **2024**, *627* (8003), 328–334. https://doi.org/10.1038/s41586-024-07117-5.